



Published in final edited form as:

*Adv Drug Deliv Rev.* 2022 October ; 189: 114505. doi:10.1016/j.addr.2022.114505.

## Image-guided intratumoral immunotherapy: Developing a clinically practical technology

Avik Som<sup>1,2</sup>, Jan-Georg Rosenboom<sup>1,2,3</sup>, Alana Chandler<sup>1,2,3</sup>, Rahul A. Sheth<sup>4</sup>, Eric Wehrenberg-Klee<sup>1</sup>

<sup>1</sup>Division of Interventional Radiology, Department of Radiology, Massachusetts General Hospital

<sup>2</sup>Koch Institute, Massachusetts Institute of Technology

<sup>3</sup>Department of Medicine, Brigham and Women's Hospital

<sup>4</sup>Department of Interventional Radiology, M.D. Anderson Cancer Center

### Abstract

Immunotherapy has revolutionized the contemporary oncology landscape, with durable responses possible across a range of cancer types. However, the majority of cancer patients do not respond to immunotherapy due to numerous immunosuppressive barriers. Efforts to overcome these barriers and increase systemic immunotherapy efficacy have sparked interest in the local intratumoral delivery of immune stimulants to activate the local immune response and subsequently drive systemic tumor immunity. While clinical evaluation of many therapeutic candidates is ongoing, development is hindered by a lack of imaging confirmation of local delivery, insufficient intratumoral drug distribution, and a need for repeated injections. The use of polymeric drug delivery systems, which have been widely used as platforms for both image guidance and controlled drug release, holds promise for delivery of intratumoral immunoadjuvants and the development of an *in situ* cancer vaccine for patients with metastatic cancer. In this review, we explore the current state of the field for intratumoral delivery and methods for optimizing controlled drug release, as well as practical considerations for drug delivery design to be optimized for clinical image guided delivery particularly by CT and ultrasound.

### Keywords

Immunotherapy; cancer vaccine; intratumoral therapy; hydrogels; CT; MRI; ultrasound

## 1. Introduction

### 1.1 Overview of immune checkpoint inhibitor therapy

Since the turn of the century, systemic immunotherapy with immune checkpoint inhibitors (ICI) has offered an exciting and powerful route for targeting cancerous cells by stimulating

---

Conflicts disclosure: AS is a consultant for Boston Scientific for an unrelated project and co-founder of CareSignal Health, a digital health company now part of Lightbeam Health. EWK acknowledges clinical and preclinical research funding as well as consulting fees from Boston Scientific, consulting fees from Sirtex, consulting fees from Embolx, advisory board for Eisai, and Delcath, cofounder and shareholder for Cytosite.

immune response through the modulation of immune checkpoints. [1,2] Under normal physiologic conditions, activation of the adaptive immune system, by for example the detection of a pathogen, concomitantly activates a series of checkpoint molecules on the immune cells. These “off switches” ensure an eventual denouement of the immune response and prevent a runaway inflammatory response. Tumors, however, capitalize on this checkpoint system by inappropriately activating these signaling pathways before the immune cells can mount an anti-tumor response. By abrogating this inhibitory mechanism, ICIs unfetter cytotoxic lymphocytes and allow for an anti-tumor response to be mounted and sustained. Multiple reviews have gone in depth through the mechanisms of ICI therapy, and a summary of the mechanism of checkpoint blockade is presented in Figure 1. [1–3]

Unfortunately, most patients will not respond to ICI treatment; the efficacy rate for ICI across the spectrum of cancer types is less than 20% (Table 1).[4] Multiple resistance mechanisms to ICI have been elucidated. For example, one potential biomarker is the tumor mutational burden; tumors with a low rate of mutations are less likely to generate unique proteins that will yield neoantigens for which a tumor-specific adaptive immune response can be generated. Furthermore, it is also clear that the pre-existing tumor immune microenvironment plays an important prognostic role in ICI efficacy. Tumors with an “immune inflamed” phenotype at baseline, characterized by T cell and myeloid cell infiltration within the tumor, are much more likely to respond to systemic immunotherapies compared to tumors that are “immune excluded” or “immune deserts” in which immune cells are marginalized at the tumor-parenchyma border or not present at all, respectively. [5,6]Adjuvant interventions that can convert the latter two phenotypes (also known as “cold” tumors) into the former (also known as “hot” tumors) have the potential to convert ICI non-responders into responders. This potential comprises the rationale behind intratumoral immunotherapy studies. [7,8]

## 1.2 Intratumoral delivery as a method to improve immunotherapy efficacy

A wide variety of approaches to increase the response rate and efficacy of checkpoint inhibitors have been tried; one of the most promising is intratumoral injection of immunotherapy. [6–9] Under this framework (Figure 2), localized injection of agents into a ‘cold’ metastasis causes an inflammatory response that modulates the baseline immunosuppressive tumor microenvironment towards an immunologically permissive state. Example intratumoral therapies include immunoadjuvant agents that activate the innate immune system, such as toll-like receptor (TLR) or stimulator of interferon gene (STING) agonists. [7] These produce an inflammatory signaling cascade that recruits dendritic cells and other antigen presenting cells to the tumor. These cells in turn present tumor antigen to cytotoxic immune cells and activate them against the tumor. Cytotoxic immune cells then migrate throughout the body to attack the tumor both at the site of immunoadjuvant injection and at distant metastases.

## 1.3 Clinical trial evaluation of intratumoral immunotherapy delivery

As of September 2021, there are 113 clinical trials of intratumoral immunotherapy, of which 68 are phase I and 57 are phase II studies (Figure 3). These studies encompass a wide range of immunotherapy-resistant tumor types and include local delivery of immunoadjuvants

such as TLR agonists, STING agonists, cytokines such as IL-2, oncolytic viruses (including engineered adenovirus, vaccinia, polio, dengue, HSV-1 among others), intratumoral injection of enriched immune cells (CAR T cell, Dendritic cell, or NK Cell therapy), often in combination with systemic or intratumoral ICI for a synergistic effect. [10] (Figure 1, left panel) Several of these trials have shown significant success. For example, the oncolytic virus talimogene laherparepvec (T-VEC), now approved for the treatment of melanoma, demonstrated a 16% durable response rate as a single agent and a 52% response rate in combination with ipilimumab compared to 23% for ipilimumab alone.[11] A phase 1 trial of intratumoral CpG oligonucleotide, a TLR9 agonist, in combination with anti-PD-1 immunotherapy demonstrated promising response rates up to 78% in 9 patients who were immunotherapy naïve. [12] Additional promising studies have included delivery of clostridium spores [13,14], and injection of dendritic cells pre-loaded with tumor cell lysate. [15,16]

#### 1.4 Challenges in intratumoral injection: controlling release and visualizing delivery

Effective intratumoral injections require precise delivery of the drug into the target lesion and may also depend on the distribution of the drug throughout tumor. The fundamental underlying assumption with intratumoral drug delivery is that by injecting the drug through a needle positioned within the tumor, the drug will be deposited within the tumor. However, we have found that this assumption is profoundly false.[17] Variations in injection technique and injection needle design, as well as tumor microenvironmental factors such as tumor interstitial pressure, can result in dramatic alterations in intratumoral drug distribution. Moreover, spillage of the drug into off-target tissues and blood vessels can result in significant systemic toxicities. In the subsequent sections, we detail specific challenges and potential solutions for intratumoral immunotherapy interventions.

**1.4.1 Limitations of imaging in intratumoral injections**—While superficial lesions can be injected by visual inspection, the majority of lesions are non-palpable and require image guidance for injection in the interventional radiology suite. The mostly widely utilized imaging modalities for intratumoral injection are CT and ultrasound, with ultrasound being favored for anything < 5 cm deep, including subcutaneous, thyroid, or breast lesions, and CT for deeper lesions and those in visceral organs. [18–23] The technique for a CT or ultrasound-guided therapeutic injection is similar to that of biopsy, which is routinely performed and accurate within a few mm of the target virtually anywhere in the body. Imaging is used to guide needle placement into tumor, but the distribution of injected intratumoral therapy within (or outside of) tumor is often unevaluable since the therapy itself cannot be visualized by the imaging modality.

Recent studies have demonstrated that image guidance is necessary to ensure accurate delivery and immune efficacy. [24,25] For example, an intratumoral drug study evaluating an iodinated compound showed CT evidence of off-target injection despite proper needle placement. [24] The majority of intratumoral drugs coming to trial cannot be visualized using standard clinical imaging techniques. This can at times impede the interpretation of clinical trial results, when leakage and diffusion away from target can contribute to non-efficacy of a drug. [10].

**1.4.1 Inadequate drug distribution**—Drug distribution is dependent on the method of administration (intravascular versus intratumoral, intratumoral injection technique, type of injection needle), the tumor environment (degree of interstitial pressure, vascular in-growth and tumor necrosis), and drug characteristics (charge, hydrophobicity, and size). These constraints have been addressed extensively to modulate chemotherapy release from controlled release formulations, and the same principles can be applied to optimizing intratumoral immunotherapy delivery. [26]

**1.4.2 Frequent need for weekly injections**—Intratumoral therapies approved or in trials often require multiple weekly injections. The requirement for multiple injections arises in part because small molecules rapidly diffuse away from the injection site on the order of minutes to hours, with variable penetration from either intravascular or intratumoral approaches.[27] To compensate and reach the therapeutic window of the agent in the desired environment, excessive levels of drug may be injected which can lead to undesired off-target side effects. Multiple weekly procedures increase the risk of bleeding and infection, and for deeper tumors requires conscious sedation with associated risks and inconvenience for the patient. They are also taxing on patients and their caregivers, as well as for the busy interventional radiology practices where most of these procedures are performed. These logistical challenges have the potential to severely limit therapeutic adoption. [28] As such, mechanisms to reduce the number of repeated injections are necessary. Extended-release technologies that have already been used for delivery of chemotherapy, such as microparticles, hydrogels or other polymeric drug carriers, may similarly enable single-administration immunotherapy treatments.[29]

## 2. Controlled release systems for intratumoral immunotherapy delivery

### 2.1 Current controlled release technology

To overcome these limitations of traditional immediate release injections, controlled release delivery mechanisms such as slow-releasing and retentive polymeric drug vehicles can help increase drug deposition and targeting as well as tracing capabilities. Figure 4 outlines different classes of injectable drug delivery formulations for chemo- and immunotherapy drugs, from micro- to nanoscale and increasing in functionality from left to right.

Going back in history, the foundation for extended-release systems was laid by macroscopic formulations that were too large to be injected, but were typically implanted, swallowed or had other administration routes. These first-generation drug release formulations relied either on diffusion from a non-degradable polymer matrix, or more commonly on the biodegradation of the excipient to liberate the drug, for which commonly degradable polymer structures such as polyesters and carbohydrates are used. For example, polylactic-co-glycolic acid (PLGA), polyglycolic acid (PGA), polycaprolactone (PCL), polyanhydrides, hydroxypropyl methylcellulose (HPMC), and cellulose acetate have been used in resorbable sutures, long-acting implants and extended-release oral formulations, and continue to be used for these applications. [29] Drug release from degradable copolymer systems can be controlled by polymer backbone properties such as the monomer chemistry, ratio of hydrophobic/hydrophilic groups, molecular weight, and crystallinity, which all affect

degradation rate and encapsulation efficiency of the drug. For example, PLGA degradation speed can be tuned from weeks to months by increasing the ratio of hydrophobic lactic acid versus the more hydrophilic glycolic acid, while polycaprolactone is more hydrophobic so it can last up to 2–3 years. [29–31]

The same or similar polymers were then later on used for microscale and injectable systems, such as PLGA- or Polyglutamic acid (PGA)-based microparticle suspensions, albeit almost exclusively for chemotherapy agents and hormones (Figure 4, left). Particulate formulations have been investigated for TLR7/8 agonists, where delivery through sub-micron particles (~300 nm) showed improved CD8 T-cell activation compared with other polymer configurations such as micelles (~10 nm), or random coils (~4 nm), but have seen little translation or clinical trials. [32,33] More recently, nano-scale linear and self-assembling polymer conjugates (Figure 4, 2<sup>nd</sup> block from left) have been used for systemic chemotherapy delivery. Conjugates are polymer backbones with functional repeat units or functional end groups that can be linked (conjugated) to drugs bearing complementary functional groups. While conjugated, the drug is inactive and becomes a “prodrug”, until the bond is cleaved (e.g., by hydrolysis in physiological setting) and the parent drug is reactivated. Such covalent linkages bear certain advantages over the free drug encapsulation described in previous technologies, such as reduced burst release, solubilization of hydrophobic drugs, high drug loadings, prolonged circulation, and enhanced tumor retention due to the large macromolecular size (EPR effect). Another benefit is a reduction in free drug levels and concomitant systemic toxicity, which otherwise in cases such as neocarzinostatin have had limited clinical translation. [34] Several polymers with functional backbones are in clinical or pre-clinical development. Examples are Opaxio / Polyglumex, a Paclitaxel-bearing backbone polyglutamic acid formulation, and DEP Docetaxel, a Docetaxel-bearing dendrimer polymer.[35–37] In general, polymer backbones with functional groups on every repeat unit open the door to co-conjugation of multiple species, for example drug combinations, or addition of targeting and imaging agents.

The majority of marketed conjugates, however, are based on PEG, which has only two end-groups available for conjugation and is non-degradable at molecular weights larger than a few thousand Daltons.[38] Here, PEG is not used as a drug-carrying backbone, but rather for its “stealth” effect that reduces immune system recognition of the agent by steric repulsion of the encapsulating shell, while increasing blood stream circulation by its increased size that evades renal clearance systems. [37] PEGylated conjugates for immunotherapy in clinical development are Pegilodecakin (Interleukin 10, anti-inflammatory cytokine), which has shown promising clinical activity when delivered systemically in combination with anti-PD-1 inhibitors [39] and NKTR-262 (intra-tumoral TLR7/8 agonist delivered with Bempegaldesleukin, a CD122 preferential IL-2 pathway agonist), that has shown good safety data and robust TLR-7/8 engagement (Figure 4).[40]

Linear polymers can also be synthesized as copolymer blocks of differing hydrophilicity, often involving PEG as the hydrophilic part and degradable polyesters such as PLGA as the hydrophobic portion, thus creating amphiphilic structures that can readily self-assemble around drug cargoes. These polymers form encapsulating nanoparticles around the active

agents, thereby increasing solubility of hydrophobic agents in aqueous formulations, limiting their systemic toxicity compared with free drugs and improving their target specificity by featuring target-binding moieties on the surface of the formed corona of the nanosphere. An example for such system to improve chemotherapy is BIND-014, which is a docetaxel-encapsulating nanoparticle decorated with functionalities that preferentially bind to prostate-cancer cell transmembrane proteins. An example for nanoparticle delivery of immunotherapy agents is SEL-068, a PLA-PEG formulation encapsulating nicotine antigen and TLR agonists as vaccine against smoking addiction (Figure 4, 3<sup>rd</sup> column).[29]

Another popular class of polymeric systems that elicit macroscale effects based on nanoscale chemistries, are hydrogels. Hydrogels are soft materials with extremely high-water content whose crosslinked polymer backbone structure allows for structural integrity while also allowing for controllable degradation, stimuli-responsiveness, biocompatibility, and controlled drug release. [29,41] Hydrogels have become a platform technology as biocompatible drug delivery systems and, unlike earlier technologies creating covalent crosslinks through toxic reagents, typically form *in situ* or before administration through the formation of non-covalent linkages. The gelling may be a result of molecular self-assembly and molecular rearrangement of polymer molecules following physiological cues such as body temperature or pH, or may be achieved by the addition of charged species, as in alginate crosslinking with Ca<sup>2+</sup> ions. Other polymer systems able to form hydrogels are certain PEG-copolymers, polyacrylamides, and polysaccharides such as alginates and carboxymethyl cellulose., such as thermosensitive An example for stimulus-induced thermogelation are low-molecular weight PLGA-PEG-PLGA copolymers, which are liquid at room temperature, allow for solubilization of hydrophobic drugs through micellar encapsulation, and form a gel at body temperatures through the increase of hydrophobic interactions (Figure 4, third panel from left). [42]

Hydrogels have been used extensively for intratumoral chemotherapy delivery where varying tumor microenvironments may affect the dwell time of the drug. [27] By producing a local depot, hydrogel injections allow for controlled sustained release of the underlying therapeutic agent to increase efficacy. [43] This technology allows significantly higher local concentrations of drug and has been further applied to intratumoral immunotherapy, for example intratumoral multi-domain peptide (MDP) hydrogel injected through a 29-gauge needle in a rat flank tumor model produced a fourfold increase in STING agonist levels locally compared to free drug where it demonstrated stimulation of the local immune environment. [44] The TransCon platform for intratumoral immunostimulatory injection uses a PEGylated hydrogel depot with a pH and temperature sensitive linker to release pro-drugs including TLR7/8 agonist resiquimod. [45–47] Hyaluronic acid (30 kDa) modified with tocopherol to facilitate nanospherical encapsulation of tocopherol-conjugated resiquimod prodrugs is another approach developed to provide long-acting intratumoral gel-like depot formation that has successfully induced tumor remission in dogs. [48] Indeed, similar to the results seen with chemotherapy release, the efficacy of intratumoral immunotherapy can be augmented by increasing the duration tumor exposure, such as by increasing the molecule size or increasing matrix binding. [49] As such, the structure of an ideal hydrogel depot would include, injectability through at least an 18 and ideally 22-gauge needle (reduces injury), controlled tuned release on the order of at least a week tuned to



the specific immunoadjuvant in question, and the ability to visualize the hydrogel during delivery.

Besides the capacity of the various polymeric carriers to encapsulate and release immunotherapy drugs, some polymers and nanoparticles have been associated with immunostimulatory potential themselves. In several studies, researchers found an immune response, such as CD8(+) and CD4(+) T-cell activation and increased presence of antibodies, in their vehicle controls similar to the adjuvanted version. Specifically, drug-free formulations involving liposomal micelles, pluronic-stabilized polypropylene sulfide NPs, Eudragit polymers, and polyanhydrides were found to elicit immunostimulatory activity. [50] These effects should be considered when designing cancer vaccines and other immunotherapies, as they have the potential to amplify but also to interfere with the *a priori* expected effect of the drug of choice. In fact, drug delivery vehicle design often involves the choice of polymers that are considered non-immunogenic, such as hyaluronic acid polymers, or acrylamide-based polymers with certain side chain functionalization. [29,51] PEG has been widely used to increase bioavailability and actually reduce immunogenicity of drugs and biologics, but concerns around PEGylated formulations being immunogenic have increased, which is a topic under investigation given the vast usage of PEG in modern drug delivery systems. [52–54]

An emerging non-polymeric approach to enable long-acting release of immunostimulatory agents utilize RNA vectors to build extended release of cytokines such as self-replicating IL-12 RNA into the cell machinery itself. [55] Additional methods to bind the delivery of the immunoadjuvants to the extracellular environment may also be a solution for prolonging release as seen by groups that have used collagen or alum-anchored immunotherapies. [56,57] Also non-aqueous but rather lipophilic formulations of TLR7/8 agonists conjugated to lipid molecules are a strategy developed to increase retention and local delivery following intratumoral injection, e.g. in sesame oil with 7.5% ethanol.[58]

## 2.2 Pre-clinical studies of hydrogels for immunotherapy

As described, there are multiple methodologies to generate controlled release intratumoral immunotherapy modalities. Hydrogels, in particular, have a long history of use as controlled release systems given their biocompatibility, injectability and a structural variety that allows for tuning of critical drug loading and releasing properties. They are amenable to being combined for both imaging, delivery and therapy with lessons that can expand to many of the other modalities. For the purpose of this review, we will focus on the hydrogel example as a platform for immunotherapy delivery and imaging. Hydrogel use for immunotherapy delivery has been recently reviewed intensively given excitement in the field, such as Huang et. al.'s review on nano, micro- and macroscale drug delivery. [59] An adaptation of their review of different gel types can be seen in Table 2. Overall, gels have used variations of intratumoral [60–63], post-surgical (tumor resection beds) [64,65], intravenous, [66–69] and subcutaneous [70–78] approaches. Subcutaneous approaches have generally attempted vaccination of tumor antigen, with multiple groups using ovalbumin as a prototype molecule. [74–78] Surgical resection allows for harvesting of unique tumor antigen which can then be used to prime the immune response. One group delivered tumor

lysate, TLR3 agonist, and gemcitabine in an implanted 5 mm disc that released 40% of the drug by 6 days [64], which increased local immunity in a breast cancer model. Another group injected CpG ODN and anti-PD-1 antibody in a nano-cocoon formed from the CpG-ODN itself with direct injection in the tumor bed. [79] These post-surgical approaches are interesting as adjuvant approaches.

However, patients with metastatic disease are unlikely to have tumor resected. Thus, several groups have evaluated controlled release of intratumorally injected immunoadjuvants (Table 2).[28] For example, one group combined anti-PD-1 antibody with Indoleamine 2,3-dioxygenase (IDO) inhibitor chemotherapy, with a release over 24 hours, which allowed for chemotherapy-induced cell death to release tumor antigen in a pro-inflammatory environment. [61] Other groups have injected immunoadjuvants, including STING agonists or OX-40, with controlled release over 15 to 30 days using supramolecular nanotubes and a nano-fluidic membrane. [62,63] Both of these approaches showed successful synergistic effect with distant metastasis reduction in brain tumors and breast cancer models.

In general, intratumorally injected immunoadjuvants were microscaled demonstrating the capability to produce a depot effect, and likely best able to be adapted for deeper percutaneous image guided approaches. In contrast, therapies dependent on intravenous systemic injection system were typically nanoscaled, taking advantage of enhanced permeation and retention or ligand targeting, and surgically implanted systems were macroscale systems requiring an incision or built for placement in the tumor bed. The wide range of tumor delivery times under controlled release with varying efficacy suggests that the ideal time period of delivery is not yet known. As discussed earlier, the minimum clinically practical time period is at least one week before requiring repeat injection, and longer time intervals are far preferable for patients and practitioners alike.

### 2.3 Challenges in intratumoral hydrogel injection: visualizing delivery

Few hydrogels delivering immunotherapy use clinically applicable imaging, with a notable exception being one group that created a Pickering emulsion of PLGA nanoparticles, anti-CTLA-4 antibodies, and ethiodized oil to create a radio-opaque injectable emulsion with the average droplet measuring  $42 \pm 5 \mu\text{m}$ . [60] Instead, fluorescence models have been used in multiple animal models to assess persistence of the drug for up to 20 days. While fluorescence is commonly used in animal models because their small size means tumors can be visualized through the skin (up to 1 cm deep), fluorophore labelled therapeutics are generally not translatable to humans where most tumors are typically far deeper.

Confirmation of intratumoral therapy delivery is key to evaluating the clinical success of clinical compounds. As a result, most clinical trials and applications have focused on superficial lesions amenable to direct optical visualization such as melanoma skin metastasis, peritoneal implants by laparoscopic surgery, or polyps/mass accessible by endoscopy, colonoscopy, or cystoscopy, or direct exam in the oral cavity, or cervix for example.

Deeper lesions not easily accessible by natural orifices has been more difficult. Based on CT imaging of the few agents that had iodinated radio-opaque compounds, several



demonstrated off-target spread, with the suggestion that the apparent efficacy of many investigational agents be compromised due to unknown leakage (Figure 5). Confirming injection led to improved distribution and intravasation of drug, dendritic cell uptake, and immune response in these trials, suggesting accurate drug delivery has important systemic implications. [44] Given the powerful local and systemic consequences of intratumoral delivery of immunotherapy agents, supporting their delivery with imaging agents is an exciting step necessary to bring these drugs to clinic. Multiple groups have begun to explore combining clinically translatable contrast agents with controlled drug delivery vehicles.

### 3. Imaging modalities available for local drug delivery

#### 3.1 Clinical Imaging Tools in Clinical Practice: cross-sectional tomography (CT), ultrasound (US), and x-ray fluoroscopy

Given the importance of being able to “see” where intratumoral delivery occurs clinically, future drug design should occur with an aim to allow visualization. As of 2021, clinically the most widespread imaging modalities in clinical use remain ultrasound[80] and CT[81] both in the United States and globally. Fluoroscopy is still widely used for angiographic and spine interventions and widely available by multiple specialties including interventional radiology, orthopedic and neurosurgery. [82–84] These modalities are relatively quick to use and available for clinicians. As such any targeted drug should ideally design for these modalities for wide-spread utilization.

Preclinical research often attaches fluorophores, but fluorescent imaging is significantly depth dependent and despite much preclinical utility over the years, has only limited clinical applications.[85,86] The vast majority of image-guided clinical intratumoral procedures use ultrasound and CT guidance, with rare specialized imaging using MRI or PET. (Figure 6) While these technologies can be difficult to scale down to the size of mice, and often more expensive than existing fluorescence options, microCT[87], small animal MRI, PET [88], and ultrasound[89] do exist and are available to the pre-clinical researcher. As the inclusion of contrast agents for each of these modalities can change pharmacokinetics of intratumorally delivered agents, factoring them into the delivery agent design is important for guiding drug delivery and successful trial outcome. For example, drug release itself is controlled by modulating hydrophobicity and hydrophilicity of the agents, porosity of hydrogels, and distribution and surface area (more in nanoparticles versus microparticles), [90] hence contrast agents may interfere with the carrier’s capability to retain or release drug. Contrast agents can vary in hydrophilicity, bulkiness, and solubility, exhibiting variable methods of clearance and safety in different compartments. Understanding these interactions, the required duration of imaging contrast, and efficacy, is integral during design itself. Below is a summary of how each tool is used clinically framed for the pre-clinical engineer.

CT scans use ionizing radiation, X-rays, to generate a tomographic image based on tissue-induced signal attenuation. The x-ray beam is absorbed (attenuated) more by structures with higher atomic numbers/electron density and increased mass density (for example calcium in bone, or iodine in iodinated contrast/ thyroid), and less so by water, or air. [91] Densities under CT scan are characterized by Hounsfield units (HU, water = 0 HU, air = -1000 HU,

bone = ~1000 HU), which are often used to identify cancer locations showing hypo- or hyperdense signals compared with surrounding tissue. [92]

CT guided interventions are performed using non-contrast exams with the patient in a recumbent position. Patients are typically under moderate sedation, although procedures may be done either with local anesthetic only and/or under anesthesia care. An initial pre-intervention axial CT image is acquired, and intravenous iodinated contrast can be given, if necessary to identify critical structures. A needle entry location is identified, the location sterilized, and local anesthetic applied. A needle is inserted and advanced under CT-imaging guidance until it is in the reached the target. (Figure 6a). Size of needle depends on the intervention to be performed, with fine needle aspirations performed through 18–22-gauge needles, core biopsies using 17–19 gauge biopsy systems, and thermal ablations using 14–16 gauge probes. Multi-side hole and multi-prong needles have also been developed but are not in routine clinical use in 2022, though they have been previously used in ethanol injection and demonstrate greater diffusion of drug delivery (Figure 6). [44]

Ultrasound provides real time and high-quality soft tissue contrast (Figure 6b). Ultrasound-guided procedures tend to be quicker than CT-guided procedures given real-time imaging feedback. Additionally, ultrasound equipment is less expensive to purchase and maintain, and does not require a dedicated technologist to operate. It uses differences in sonographic reflections to distinguish tissues. For example, water is generally hypoechoic, whereas fat is hyperechoic. Ultrasound cannot visualize through air or bone. Intravascular contrast using microbubbles can be used to allow contrast enhancement temporarily as well over the same time duration as seen using CT visible iodinated contrast (Figure 6d). [93]

For ultrasound guided interventions, the patient is oriented to allow for the shortest distance to the target. After a similar sterile preparation and delivery of local anesthetic, the needle is followed to the target under active real-time ultrasound guidance.

Many lesions within the kidney, liver, peritoneum or pleura may be amenable to both ultrasound and CT depending on the exact imaging characteristics of the lesions. [94–96] Of note, contrast agents delivered to the site, generally should clear prior to subsequent staging exams as hyperdense objects such as metal or barium have significant streak artifact that limits response assessment. [97,98]

In the context of cancer therapy, fluoroscopy is most commonly used for intra-arterial therapies, most commonly liver-directed delivery of radiation (Yttrium 90) or chemotherapy-saturated beads. [99,100] Figure 6c. Fluoroscopy heavily uses contrast injections to allow real time assessments of catheter locations and interventions through the vasculature, which can be used to assess therapeutic delivery. In these methods, combinations with ethiodol within microbeads such as the Lumi© beads from Boston Scientific have been used in the past to confirm target delivery, or in mixtures with contrast during injection at the bedside table. [101,102]

### 3.2 Uncommon clinical interventional techniques: MRI, PET, and Optical Imaging

Magnetic resonance imaging-guided procedures are time-intensive and thus not considered a cost-effective use of an MRI scanner by most radiology practices. MRI interventions are used in select instances where CT or US is deemed insufficient for adequate guidance and predominantly by research institutions. Where used MRI has been applied for both drug delivery but also in the use of MR thermometry to evaluate ablation. [103,104] MR-guided focal ultrasound for prostate ablation is an example that has begun to be used for prostate ablations and may provide future promise as the field grows (Figure 7 a). [105] Similarly PET imaging, has been used more as a planning study with fusion as opposed to live imaging. [106,107] Access to an FDG-PET guided intervention is not yet widespread, though has been reported in case series to increase biopsy yield (Figure 7b). [106–108] Labelling intratumoral therapeutics with radioactivity for purposes of imaging adds significant logistical issues of production, limiting operator exposure, and overall radiation safety that significantly limits adoption. Near-infrared fluorescent imaging has not had wide-spread adoption due to limited depth penetration. Applications are primarily surgical, for example for laparoscopic surgery or in the optical fields of cystoscopy or endoscopy, often currently looking at vascularization of the lesions, the common bile duct, or lymphatics. [85,86] These applications remain limited significantly by depth of visualization and can be combined with use of ultrasound (such as endoscopic ultrasound or laparoscopic ultrasound), or with fluoroscopy as is done with fiducial guided lung resections. Applications in fluorescence imaging to aid percutaneous intervention radiology techniques remain experimental (Figure 7c). [109]

### 3.3 Materials for enabling contrast on imaging.

**3.3.1 Non-permanent contrast for CT imaging**—Iodinated contrast is the mainstay for increased contrast visualization particularly to look at enhancement of lesions. Concentrations for radio-opacity are typically in the 100 mgI/mL range and can be mixed in at 10–50% v/v intravenously. The structure of the iodinated components is shown in Figure 8a. [110] For combination into polymers, most iodinated compounds have a hydroxyl group that can be used for chemical conjugation or be combined using hydrophobic/hydrophilic characteristics for steric combination into polymer conjugates. For intratumoral injection, non-permanent contrast is recommended, as permanent contrast agents can complicate future response assessment. The retention of iodinated contrast depends on both the iodinated contrast used and how it is delivered. For example, groups have shown an end-hole injection into a flank model has dispersion of iohexol within 5 minutes while a multi-side hole injection offers greater retention. [44] In a study of hysterosalpingograms, injection of lipiodol (oil-soluble contrast) had a half-life of 50 days whereas iotrolan, a water-soluble agent, was fully excreted in 2 days.[111] For confirmation of target delivery during the procedure, retention within tumor of approximately an hour is necessary. However, for purposes of understanding drug-release kinetics, it is much better for the imaging contrast release profile to match the expected release rate drug.

**3.3.3 Ultrasound agents for imaging**—Ultrasound examination have used microbubbles to increase echogenicity, thereby providing increased contrast within injected structures upon administration. Lipid encasing microbubbles have been used to add

functionality and even enable drug delivery. [112] (Figure 8b) Applications can often be multimodality and be both radio-opaque and echogenic as the modalities tend to be orthogonal to each other. Interval echogenicity assessment allows follow-up of gel degradation. [112,113] Given the convenience of ultrasound globally, building in this capability for polymeric drug delivery systems dramatically increases the reach for appropriate injection and therapy broadly around the world.

### 3.4 Hydrogels containing imaging contrast

Multiple groups have taken advantage of the above knowledge to create contrast-containing hydrogels that can deliver therapeutic compounds under image guidance. Several reviews have delved deeply into possible techniques. [114,115] A review of various polymeric formulations for imaging via an investigational MRI technique, chemical exchange saturation transfer (CEST-MRI), fluorescence, and CT has been adapted here with a particular focus on drug release and method of utilizing imaging contrast as examples of what could possibly be done with immunotherapy. (Table 3)

Hydrogels can be built where the polymer itself provides contrast. Examples include alginate and hyaluronic acid in the setting of CEST-MRI. [116–118] However, CEST-MRI is not in current clinical use outside of focused MR spectroscopy. The lack of widescale use reduces the utility of this technique for drug delivery and monitoring, particularly on a visualization scale. Similarly, fluorescence-based methods [119–126] are difficult to be applied for anything but surgical applications with direct camera visualization.

CT, as a fast and widespread modality, provides the highest translatability. Among examples of already developed CT-imageable hydrogels, groups have used physical loading of gold nanoparticle into hydrogels made of gelatin-tyramine or alginate [127], or a PNAGA-PAAm copolymer [128]. These conjugates were evaluated for the intratumoral delivery of chemotherapies and would be interesting to explore for immunoadjuvants as well, with the caveat that gold would be retained as a permanent contrast agent, leading to potential treatment assessment problems from streak artifact.

Approved iodinated contrast agents are designed to be highly water soluble and thus difficult to load directly into hydrogels without washing out. Groups have tackled this by incorporating iodine into the hydrogel backbone [129]. Microbeads with iodinated contrast have been used as intravascular contrast agents during chemoembolization delivery [130,131]. Duration of contrast ranges from a few hours to 12 days for degradable systems, roughly enough time to determine localization, but unlikely to cause issues with follow-up imaging, where contrast retention may complicate response assessment. Ultrasound microbubbles take advantage of intrinsic contrast from air in the bubble which makes the gel hyperechogenic and have been used to visualize degradation [132].

Imageable hydrogels developed to date have generally been used to deliver hydrophobic chemotherapies, such as doxorubicin or paclitaxel, however the underlying technologies are directly applicable for checkpoint inhibitors and immunotherapy adjuvants. For example, the combination Pickering emulsion of ethiodized oil and PLGA nanoparticles delivering anti-CTLA-4 is a clear example of an intratumoral delivery agent combining both mechanisms

[60]. In particular, the CT technologies discussed previously, including adding iodinated compounds to polymer backbone or high Z particles like gold into the depots show promise and likely applicability to immunoadjuvant delivery as already described that had otherwise used primarily fluorescence to show delivery in pre-clinical animal models. Of note, few of the delivery mechanisms have optimized for aligning visualization duration with drug release curve and as such primarily confirm delivery. This is potentially useful for avoiding long term contrast related streak artifacts. However, being able to see the drug's duration and pharmacokinetics may be useful for therapy planning. In an assessment of currently running clinical trials of intratumoral immunotherapy agent, only one compound, Rose Bengal Disodium, which has iodine in its chemical composition, was able to be tracked. Future studies creating image guided controlled release technologies would be ideal for confirming both delivery and visualizing real time pharmacokinetics of therapy. [17]

## Summary

Immunotherapy, the technology that has brought the hope of a cure for a subset of patients with metastatic disease, continues to spur significant interest in developing methods for overcoming resistance. Intratumoral delivery of immunoadjuvants is an area of active and fertile clinical investigation, and clinical experience to date has taught us that this nascent fields' success will increase with both controlled drug release profiles that reduce the number of procedures necessary as well as the ability to visually confirm target-delivery and drug-release kinetics. For the practitioner and engineer, intratumoral delivery requires development of delivery platforms that can be seen easily in near real-time, particularly under CT, ultrasound, or X-ray fluoroscopy. Biocompatible polymers provide a toolbox to build suitable delivery vehicles for intratumoral immunoadjuvants, ranging from particle suspensions and polymer-drug-conjugates to amphiphilic block-polymers that self-assemble into nanoparticles. These polymers can allow the solubilization of hydrophobic compounds, encapsulation of imaging agents, increased drug load, specific tissue-targeting capabilities and the control of release patterns over time. Some of these technologies, such as nano-encapsulating hydrogels, can provide platform technologies, however, given the complexity of immunotherapy agent chemistries, their optimal range of efficacy, and the targeted organs, an individual formulation for each scenario is still required. Especially in conjunction with the incorporation of imaging agents, a better understanding of the change in delivery performance as a function of formulating certain drugs and imaging agents into polymeric systems is required to speed up formulation efforts. In this review, we have underlined some of the existing technologies that have been utilized for image-guided delivery as well as controlled release of immunotherapy.

## Acknowledgments:

We would like to acknowledge the help of Dr. Giovanni Traverso for their aid with figure development and advice for this work.

## Funding Support:

EWK acknowledges support from NIH/NCI K08CA245257, AS acknowledges support from the RSNA Resident Research Award. JGR acknowledges funding from the Bill & Melinda Gates Foundation.

## Abbreviation

<b>CT</b>	computed tomography
<b>MRI</b>	magnetic resonance imaging

## References

- [1]. Wei S, Duffy C, Allison J, Fundamental Mechanisms of Immune Checkpoint Blockade Therapy \_ Enhanced Reader, *Cancer Discovery*. (2018) 1069–1086. 10.1158/2159-8290.CD-18-0367. [PubMed: 30115704]
- [2]. Granier C, de Guillebon E, Blanc C, Roussel H, Badoual C, Colin E, Saldmann A, Gey A, Oudard S, Tartour E, Mechanisms of action and rationale for the use of checkpoint inhibitors in cancer, *ESMO Open*. 2 (2017). 10.1136/esmoopen-2017-000213.
- [3]. Seidel JA, Otsuka A, Kabashima K, Anti-PD-1 and anti-CTLA-4 therapies in cancer: Mechanisms of action, efficacy, and limitations, *Frontiers in Oncology*. 8 (2018). 10.3389/fonc.2018.00086.
- [4]. Haslam A, Prasad V, Estimation of the Percentage of US Patients With Cancer Who Are Eligible for and Respond to Checkpoint Inhibitor Immunotherapy Drugs, *JAMA Netw Open*. 2 (2019) e192535. 10.1001/jamanetworkopen.2019.2535. [PubMed: 31050774]
- [5]. Sade-Feldman M, Jiao YJ, Chen JH, Rooney MS, Barzily-Rokni M, Eliane JP, Bjorgaard SL, Hammond MR, Vitzthum H, Blackmon SM, Frederick DT, Hazar-Rethinam M, Nadres BA, van Seventer EE, Shukla SA, Yizhak K, Ray JP, Rosebrock D, Livitz D, Adalsteinnsson V, Getz G, Duncan LM, Li B, Corcoran RB, Lawrence DP, Stemmer-Rachamimov A, Boland GM, Landau DA, Flaherty KT, Sullivan RJ, Hacohen N, Resistance to checkpoint blockade therapy through inactivation of antigen presentation, *Nature Communications*. 8 (2017). 10.1038/s41467-017-01062-w.
- [6]. Jenkins R, Barbie D, Flaherty K, Mechanisms of resistance to immune checkpoint inhibitors, (n.d.).
- [7]. Hamid O, Ismail R, Puzanov I, Intratumoral Immunotherapy—Update 2019, *The Oncologist*. 25 (2020). 10.1634/theoncologist.2019-0438.
- [8]. Marabelle A, Tselikas L, de Baere T, Houot R, Intratumoral immunotherapy: Using the tumor as the remedy, *Annals of Oncology*. 28 (2017) xii33–xii43. 10.1093/annonc/mdx683. [PubMed: 29253115]
- [9]. Goldberg EP, Hadba AR, Almond BA, Marotta JS, Intratumoral cancer chemotherapy and immunotherapy: opportunities for nonsystemic preoperative drug delivery, *Journal of Pharmacy and Pharmacology*. 54 (2010) 159–180. 10.1211/0022357021778268.
- [10]. Melero I, Castanon E, Alvarez M, Champiat S, Marabelle A, Intratumoural administration and tumour tissue targeting of cancer immunotherapies, *Nature Reviews Clinical Oncology* 2021 18:9. 18 (2021) 558–576. 10.1038/s41571-021-00507-y.
- [11]. Chesney J, Puzanov I, Collichio F, Singh P, Milhem MM, Glaspy J, Hamid O, Ross M, Friedlander P, Garbe C, Logan TF, Hauschild A, Lebbé C, Chen L, Kim JJ, Gansert J, Andtbacka RHI, Kaufman HL, Randomized, Open-Label Phase II Study Evaluating the Efficacy and Safety of Talimogene Laherparepvec in Combination With Ipilimumab Versus Ipilimumab Alone in Patients With Advanced, Unresectable Melanoma, *J Clin Oncol*. 36 (2018) 1658–1667. 10.1200/JCO.2017.73.7379. [PubMed: 28981385]
- [12]. Ribas A, Medina T, Kummer S, Amin A, Kalbasi A, Drabick JJ, Barve M, Daniels GA, Wong DJ, Schmidt E. v, Candia AF, Coffman RL, Leung ACF, Janssen RS, Sd-101 in combination with pembrolizumab in advanced melanoma: Results of a phase Ib, multicenter study, *Cancer Discovery*. 8 (2018). 10.1158/2159-8290.CD-18-0280.
- [13]. Janku F, Zhang HH, Pezeshki A, Goel S, Murthy R, Wang-Gillam A, Shepard DR, Helgason T, Masters T, Hong DS, Piha-Paul SA, Karp DD, Klang M, Huang SY, Sakamuri D, Raina A, Torrisi J, Solomon SB, Weissfeld A, Trevino E, DeCrescenzo G, Collins A, Miller M, Salstrom JL, Korn RL, Zhang L, Saha S, Leontovich AA, Tung D, Kreider B, Varterasian M, Khazaie K, Gounder MM, Intratumoral Injection of Clostridium novyi-NT Spores in Patients



with Treatment-refractory Advanced Solid Tumors, *Clinical Cancer Research*. 27 (2021) 96–106. 10.1158/1078-0432.CCR-20-2065. [PubMed: 33046513]

- [14]. Roberts NJ, Zhang L, Janku F, Collins A, Bai R-Y, Staedtke V, Rusk AW, Tung D, Miller M, Roix J, Khanna K. v, Murthy R, Benjamin RS, Helgason T, Szvalb AD, Bird JE, Roy-Chowdhuri S, Zhang HH, Qiao Y, Karim B, McDaniel J, Elpiner A, Sahara A, Lachowicz J, Phillips B, Turner A, Klein MK, Post G, Diaz LA Jr., Riggins GJ, Papadopoulos N, Kinzler KW, Vogelstein B, Bettegowda C, Huso DL, Varterasian M, Saha S, Zhou S, Intratumoral injection of *Clostridium novyi*-NT spores induces antitumor responses, *Sci Transl Med*. 6 (2014) 249ra111. 10.1126/SCITRANSLMED.3008982.
- [15]. Finkelstein SE, Iclozan C, Bui MM, Cotter MJ, Ramakrishnan R, Ahmed J, Noyes DR, Cheong D, Gonzalez RJ, Heysek RV, Berman C, Lenox BC, Janssen W, Zager JS, Sondak VK, Letson GD, Antonia SJ, Gabrilovich DI, Combination of external beam radiotherapy (EBRT) with intratumoral injection of dendritic cells as neo-adjuvant treatment of high-risk soft tissue sarcoma patients, *Int J Radiat Oncol Biol Phys*. 82 (2012) 924–932. 10.1016/J.IROBP.2010.12.068. [PubMed: 21398051]
- [16]. Raj S, Bui MM, Springett G, Conley A, Lavilla-Alonso S, Zhao X, Chen D, Haysek R, Gonzalez R, Letson GD, Finkelstein SE, Chiappori AA, Gabrilovitch DI, Antonia SJ, Long-term clinical responses of neoadjuvant dendritic cell infusions and radiation in soft tissue sarcoma, *Sarcoma*. 2015 (2015). 10.1155/2015/614736.
- [17]. Sheth RA, Murthy R, Hong DS, Patel S, Overman MJ, Diab A, Hwu P, Tam A, Assessment of Image-Guided Intratumoral Delivery of Immunotherapeutics in Patients with Cancer, *JAMA Network Open*. 3 (2020). 10.1001/jamanetworkopen.2020.7911.
- [18]. Smith T, Kaufman C, Ultrasound guided thyroid biopsy, *Techniques in Vascular and Interventional Radiology*. (2021) 100768. 10.1016/J.TVIR.2021.100768. [PubMed: 34861967]
- [19]. BD F, JD C, CL D, Ultrasound-guided needle biopsy of the breast and other interventional procedures., *Radiologic Clinics of North America*. 30 (1992) 167–185. <https://europepmc.org/article/med/1732925> (accessed October 24, 2021). [PubMed: 1732925]
- [20]. Wu CC, Maher MM, Shepard J-AO, CT-Guided Percutaneous Needle Biopsy of the Chest: Preprocedural Evaluation and Technique, 10.2214/AJR.10.4657. 196 (2012). 10.2214/AJR.10.4657.
- [21]. Gupta S, Nguyen HL, Frank A J. Ahrar Morello, K, Wallace MJ, Madoff DC, Murthy R, Hicks ME, Various Approaches for CT-guided Percutaneous Biopsy of Deep Pelvic Lesions: Anatomic and Technical Considerations1, 10.1148/Rg.241035063. 24 (2004) 175–189. 10.1148/RG.241035063.
- [22]. Thanos L, Zorpala A, Papaioannou G, Malagari K, Brountzos E, Kelekis D, Safety and efficacy of percutaneous CT-guided liver biopsy using an 18-gauge automated needle, *European Journal of Internal Medicine*. 16 (2005) 571–574. 10.1016/J.EJIM.2005.06.010. [PubMed: 16314238]
- [23]. Ko KH, Huang TW, Lee SC, Chang WC, Gao HW, Hsu HH, A simple and efficient method to perform preoperative pulmonary nodule localization: CT-guided patent blue dye injection, *Clinical Imaging*. 58 (2019) 74–79. 10.1016/j.clinimag.2019.06.015. [PubMed: 31279987]
- [24]. Sheth RA, Murthy R, Hong DS, Patel S, Overman MJ, Diab A, Hwu P, Tam A, Assessment of Image-Guided Intratumoral Delivery of Immunotherapeutics in Patients with Cancer, *JAMA Network Open*. 3 (2020). 10.1001/jamanetworkopen.2020.7911.
- [25]. Tselikas L, Champiat S, Sheth RA, Yevich S, Ammari S, Deschamps F, Farhane S, Roux C, Susini S, Mouraud S, Delpla A, Raoult T, Robert C, Massard C, Barlesi F, Soria JC, Marabelle A, de Baere T, Interventional radiology for local immunotherapy in oncology, *Clinical Cancer Research*. 27 (2021) 2698–2705. 10.1158/1078-0432.CCR-19-4073. [PubMed: 33419781]
- [26]. Huang A, Pressnall MM, Lu R, Huayamares SG, Griffin JD, Groer C, DeKosky BJ, Forrest ML, Berkland CJ, Human intratumoral therapy: Linking drug properties and tumor transport of drugs in clinical trials, *Journal of Controlled Release*. 326 (2020) 203–221. 10.1016/j.jconrel.2020.06.029. [PubMed: 32673633]
- [27]. Minchinton AI, Tannock IF, Drug penetration in solid tumours, *Nature Reviews Cancer*. 6 (2006) 583–592. 10.1038/NRC1893. [PubMed: 16862189]

- [28]. Hong WX, Haebe S, Lee AS, Benedikt Westphalen C, Norton JA, Jiang W, Levy R, Intratumoral immunotherapy for early-stage solid tumors, *Clinical Cancer Research*. 26 (2020) 3091–3099. 10.1158/1078-0432.CCR-19-3642. [PubMed: 32071116]
- [29]. Kamaly N, Yameen B, Wu J, Farokhzad OC, Degradable Controlled-Release Polymers and Polymeric Nanoparticles: Mechanisms of Controlling Drug Release, *Chem Rev*. 116 (2016) 2602. 10.1021/ACS.CHEMREV.5B00346. [PubMed: 26854975]
- [30]. Babae S, Pajovic S, Kirtane AR, Shi J, Caffarel-Salvador E, Hess K, Collins JE, Tamang S, Wahane A. v, Hayward AM, Mazdiyasi H, Langer R, Traverso G, Temperature-responsive biometamaterials for gastrointestinal applications, *Science Translational Medicine*. 11 (2019). 10.1126/SCITRANSLMED.AAU8581/SUPPL\_FILE/AAU8581\_SM.PDF.
- [31]. Kirtane AR, Abouzid O, Minahan D, Bense T, Hill AL, Selinger C, Bershteyn A, Craig M, Mo SS, Mazdiyasi H, Cleveland C, Rogner J, Lee YAL, Booth L, Javid F, Wu SJ, Grant T, Bellinger AM, Nikolic B, Hayward A, Wood L, Eckhoff PA, Nowak MA, Langer R, Traverso G, Development of an oral once-weekly drug delivery system for HIV antiretroviral therapy, *Nature Communications* 2017 9:1. 9 (2018) 1–12. 10.1038/s41467-017-02294-6.
- [32]. Lynn GM, Chytil P, Francica JR, Lagová A, Kueberuwa G, Ishizuka AS, Zaidi N, Ramirez-Valdez RA, Blobel NJ, Baharom F, Leal J, Wang AQ, Germer MY, Etrych T, Ulbrich K, Seymour LW, Seder RA, Laga R, Impact of Polymer-TLR-7/8 Agonist (Adjuvant) Morphology on the Potency and Mechanism of CD8 T Cell Induction, *Biomacromolecules*. 20 (2019) 854–870. 10.1021/ACS.BIOMAC.8B01473/SUPPL\_FILE/BM8B01473\_SI\_001.PDF. [PubMed: 30608149]
- [33]. Bhagchandani S, Johnson JA, Irvine DJ, Evolution of Toll-like receptor 7/8 agonist therapeutics and their delivery approaches: From antiviral formulations to vaccine adjuvants, *Advanced Drug Delivery Reviews*. 175 (2021) 113803. 10.1016/J.ADDR.2021.05.013. [PubMed: 34058283]
- [34]. Maeda H, SMANCS and polymer-conjugated macromolecular drugs: advantages in cancer chemotherapy, *Advanced Drug Delivery Reviews*. 46 (2001) 169–185. 10.1016/S0169-409X(00)00134-4. [PubMed: 11259839]
- [35]. Larson N, Ghandehari H, Polymeric Conjugates for Drug Delivery, *Chemistry of Materials*. 24 (2012) 840–853. 10.1021/CM2031569. [PubMed: 22707853]
- [36]. Greco F, Vicent MJ, Combination therapy: Opportunities and challenges for polymer–drug conjugates as anticancer nanomedicines, *Advanced Drug Delivery Reviews*. 61 (2009) 1203–1213. 10.1016/J.ADDR.2009.05.006. [PubMed: 19699247]
- [37]. Ekladius I, Colson YL, Grinstaff MW, Polymer-drug conjugate therapeutics: advances, insights and prospects, *Nat Rev Drug Discov*. 18 (2019) 273–294. 10.1038/S41573-018-0005-0. [PubMed: 30542076]
- [38]. Kawai F, Biodegradation of Polyethers (Polyethylene Glycol, Polypropylene Glycol, Polytetramethylene glycol, and Others), *Biopolymers Online*. (2001). 10.1002/3527600035.BPOL9012.
- [39]. Tannir NM, Papadopoulos KP, Wong DJ, Aljumaily R, Hung A, Afable M, Kim JS, Ferry D, Drakaki A, Bendell J, Naing A, Pegilodecakin as monotherapy or in combination with anti-PD-1 or tyrosine kinase inhibitor in heavily pretreated patients with advanced renal cell carcinoma: Final results of cohorts A, G, H and I of IVY Phase I study, *Int J Cancer*. 149 (2021) 403–408. 10.1002/IJC.33556. [PubMed: 33709428]
- [40]. Diab A, Curti B, Bilén M, Brohl A, Domingo-Musibay E, Borazanci E, Fanton C, Haglund C, Vimal M, Muhsin M, Marcondes M, Nguyen A, Tagliaferri M, Lin W, Zalevsky J, D'Angelo S, 368 REVEAL: Phase 1 dose-escalation study of NKTR-262, a novel TLR7/8 agonist, plus bempegaldesleukin: local innate immune activation and systemic adaptive immune expansion for treating solid tumors, *Journal for ImmunoTherapy of Cancer*. 8 (2020) A224.2–A225. 10.1136/JITC-2020-SITC2020.0368.
- [41]. Dong YC, Bouché M, Uman S, Burdick JA, Cormode DP, Detecting and Monitoring Hydrogels with Medical Imaging, *ACS Biomaterials Science and Engineering*. 7 (2021) 4027–4047. 10.1021/acsbomaterials.0c01547. [PubMed: 33979137]
- [42]. Ghahremankhani AA, Dorkoosh F, Dinarvand R, PLGA-PEG-PLGA tri-block copolymers as in situ gel-forming peptide delivery system: effect of formulation properties on peptide release, *Pharm Dev Technol*. 13 (2008) 49–55. 10.1080/10837450701702842. [PubMed: 18300099]

- [43]. Fakhari A, Anand Subramony J, Engineered in-situ depot-forming hydrogels for intratumoral drug delivery, *Journal of Controlled Release*. 220 (2015) 465–475. [PubMed: 26585504]
- [44]. Muñoz NM, Williams M, Dixon K, Dupuis C, McWatters A, Avritscher R, Manrique SZ, McHugh K, Murthy R, Tam A, Naing A, Patel SP, Leach D, Hartgerink JD, Young S, Prakash P, Hwu P, Sheth RA, Influence of injection technique, drug formulation and tumor microenvironment on intratumoral immunotherapy delivery and efficacy, *Journal for Immunotherapy of Cancer*. 9 (2021). 10.1136/JITC-2020-001800.
- [45]. Karpf DB, Pihl S, Mourya S, Mortensen E, Kovoor E, Markova D, Leff JA, A Randomized Double-Blind Placebo-Controlled First-In-Human Phase 1 Trial of TransCon PTH in Healthy Adults, *Journal of Bone and Mineral Research*. 35 (2020) 1430–1440. 10.1002/JBMR.4016. [PubMed: 32212275]
- [46]. A Study of TransCon TLR7/8 Agonist With or Without Pembrolizumab in Patients With Advanced or Metastatic Solid Tumors - Full Text View - [ClinicalTrials.gov](https://clinicaltrials.gov/ct2/show/NCT04799054), (n.d.). <https://clinicaltrials.gov/ct2/show/NCT04799054> (accessed June 13, 2022).
- [47]. Mirza A, Zuniga L, Uppal K, Bang K, Hong E, Sabharwal S, Lee Y, Martinez S, Rosen D, Punnonen J, 16 Tumor growth inhibition mediated by a single dose of intratumoral TransCon™ TLR7/8 agonist was associated with activated circulating T and B cells and sustained low levels of systemic cytokines, *Journal for Immunotherapy of Cancer*. 9 (2021) A18–A18. 10.1136/JITC-2021-SITC2021.016.
- [48]. Lu R, Groer C, Kleindl PA, Moulder KR, Huang A, Hunt JR, Cai S, Aires DJ, Berkland C, Forrest ML, Formulation and preclinical evaluation of a Toll-like receptor 7/8 agonist as an anti-tumoral immunomodulator, *J Control Release*. 306 (2019) 165. 10.1016/J.JCONREL.2019.06.003. [PubMed: 31173789]
- [49]. Momin N, Palmeri JR, Lutz EA, Jailkhani N, Mak H, Tabet A, Chinn MM, Kang BH, Spanoudaki V, Hynes RO, Wittrup KD, Maximizing response to intratumoral immunotherapy in mice by tuning local retention. *Nat Commun*. 13 (2022). 10.1038/S41467-021-27390-6.
- [50]. Batty CJ, Tiet P, Bachelder EM, Ainslie KM, Drug Delivery for Cancer Immunotherapy and Vaccines, *Pharm Nanotechnol*. 6 (2018) 232–244. 10.2174/2211738506666180918122337. [PubMed: 30227827]
- [51]. Scales CW, Huang F, Li N, Vasilieva YA, Ray J, Convertine AJ, McCormick CL, Corona-stabilized interpolyelectrolyte complexes of siRNA with nonimmunogenic, hydrophilic/cationic block copolymers prepared by aqueous RAFT polymerization, *Macromolecules*. 39 (2006) 6871–6881. 10.1021/MA061453C/SUPPL\_FILE/MA061453CSI20060628\_044849.PDF.
- [52]. Schellekens H, Hennink WE, Brinks V, The Immunogenicity of Polyethylene Glycol: Facts and Fiction, *Pharmaceutical Research* 2013 30:7. 30 (2013) 1729–1734. 10.1007/S11095-013-1067-7.
- [53]. Kozma GT, Shimizu T, Ishida T, Szebeni J, Anti-PEG antibodies: Properties, formation, testing and role in adverse immune reactions to PEGylated nano-biopharmaceuticals, *Advanced Drug Delivery Reviews*. 154–155 (2020) 163–175. 10.1016/J.ADDR.2020.07.024.
- [54]. Shiraishi K, Yokoyama M, Toxicity and immunogenicity concerns related to PEGylated-micelle carrier systems: a review, <http://www.tandfonline.com/Action/JournalInformation?Show=aimsScope&journalCode=tsta20#.VmBmuzZFCUk>. 20 (2019) 324–336. 10.1080/14686996.2019.1590126.
- [55]. Li Y, Su Z, Zhao W, Zhang X, Momin N, Zhang C, Wittrup KD, Dong Y, Irvine DJ, Weiss R, Multifunctional oncolytic nanoparticles deliver self-replicating IL-12 RNA to eliminate established tumors and prime systemic immunity, *Nat Cancer*. 1 (2020) 882–893. 10.1038/S43018-020-0095-6. [PubMed: 34447945]
- [56]. Agarwal Y, Milling LE, Chang JYH, Santollani L, Sheen A, Lutz EA, Tabet A, Stinson J, Ni K, Rodrigues KA, Moyer TJ, Melo MB, Irvine DJ, Wittrup KD, Intratumorally injected alum-tethered cytokines elicit potent and safer local and systemic anticancer immunity, *Nat Biomed Eng*. 6 (2022) 129–143. 10.1038/S41551-021-00831-9. [PubMed: 35013574]
- [57]. Momin N, Palmeri JR, Lutz EA, Jailkhani N, Mak H, Tabet A, Chinn MM, Kang BH, Spanoudaki V, Hynes RO, Wittrup KD, Maximizing response to intratumoral immunotherapy in mice by tuning local retention. *Nat Commun*. 13 (2022). 10.1038/S41467-021-27390-6.

- [58]. Mullins SR, Vasilakos JP, Deschler K, Grigsby I, Gillis P, John J, Elder MJ, Swales J, Timosenko E, Cooper Z, Dovedi SJ, Leishman AJ, Luheshi N, Elvecrog J, Tilahun A, Goodwin R, Herbst R, Tomai MA, Wilkinson RW, Intratumoral immunotherapy with TLR7/8 agonist MEDI9197 modulates the tumor microenvironment leading to enhanced activity when combined with other immunotherapies, *Journal for ImmunoTherapy of Cancer*. 7 (2019) 244. 10.1186/S40425-019-0724-8. [PubMed: 31511088]
- [59]. Huang P, Wang X, Liang X, Yang J, Zhang C, Kong D, Wang W, Nano-, micro-, and macroscale drug delivery systems for cancer immunotherapy, *Acta Biomaterialia*. 85 (2019) 1–26. 10.1016/J.ACTBIO.2018.12.028. [PubMed: 30579043]
- [60]. Tselikas L, de Baere T, Isoardo T, Susini S, Ser-Le Roux K, Polrot M, Adam J, Rouanne M, Zitvogel L, Moine L, Deschamps F, Marabelle A, Pickering emulsions with ethiodized oil and nanoparticles for slow release of intratumoral anti-CTLA4 immune checkpoint antibodies, *J Immunother Cancer*. 8 (2020) 579. 10.1136/jitc-2020-000579.
- [61]. Yu S, Wang C, Yu J, Wang J, Lu Y, Zhang Y, Zhang X, Hu Q, Sun W, He C, Chen X, Gu Z, Injectable Bioresponsive Gel Depot for Enhanced Immune Checkpoint Blockade, *Advanced Materials*. 30 (2018) 1801527. 10.1002/ADMA.201801527.
- [62]. Wang F, Su H, Xu D, Dai W, Zhang W, Wang Z, Anderson CF, Zheng M, Oh R, Wan F, Cui H, Tumour sensitization via the extended intratumoural release of a STING agonist and camptothecin from a self-assembled hydrogel, *Nature Biomedical Engineering* 2020 4:11. 4 (2020) 1090–1101. 10.1038/s41551-020-0597-7.
- [63]. Chua CYX, Jain P, Susnjar A, Rhudy J, Folci M, Ballerini A, Gilbert A, Singh S, Bruno G, Filgueira CS, Yee C, Butler EB, Grattoni A, Nanofluidic drug-eluting seed for sustained intratumoral immunotherapy in triple negative breast cancer, *J Control Release*. 285 (2018) 23–34. 10.1016/J.JCONREL.2018.06.035. [PubMed: 30008369]
- [64]. Phuengkham H, Song C, SH. Um, YT. Lim, Implantable Synthetic Immune Niche for Spatiotemporal Modulation of Tumor-Derived Immunosuppression and Systemic Antitumor Immunity: Postoperative Immunotherapy, *Adv Mater*. 30 (2018). 10.1002/ADMA.201706719.
- [65]. Wang C, Wang X, Dong K, Luo J, Zhang Q, Cheng Y, Injectable and responsively degradable hydrogel for personalized photothermal therapy, *Biomaterials*. 104 (2016) 129–137. 10.1016/J.BIOMATERIALS.2016.07.013. [PubMed: 27449949]
- [66]. Cheng K, Ding Y, Zhao Y, Ye S, Zhao X, Zhang Y, Ji T, Wu H, Wang B, GJ. Anderson, L. Ren, G. Nie, Sequentially Responsive Therapeutic Peptide Assembling Nanoparticles for Dual-Targeted Cancer Immunotherapy, *Nano Lett*. 18 (2018) 3250–3258. 10.1021/ACS.NANOLETT.8B01071. [PubMed: 29683683]
- [67]. Park J, Wrzesinski SH, Stern E, Look M, Criscione J, Ragheb R, Jay SM, Demento SL, Agawu A, Licona Limon P, Ferrandino AF, Gonzalez D, Habermann A, Flavell RA, Fahmy TM, Combination delivery of TGF- $\beta$  inhibitor and IL-2 by nanoscale liposomal polymeric gels enhances tumour immunotherapy, *Nat Mater*. 11 (2012) 895–905. 10.1038/NMAT3355. [PubMed: 22797827]
- [68]. Zhu M, Ding X, Zhao R, Liu X, Shen H, Cai C, Ferrari M, Wang HY, Wang RF, Co-delivery of tumor antigen and dual toll-like receptor ligands into dendritic cell by silicon microparticle enables efficient immunotherapy against melanoma, *Journal of Controlled Release*. 272 (2018) 72–82. 10.1016/J.JCONREL.2018.01.004. [PubMed: 29325699]
- [69]. Chen Q, Xu L, Liang C, Wang C, Peng R, Liu Z, Photothermal therapy with immune-adjuvant nanoparticles together with checkpoint blockade for effective cancer immunotherapy, *Nature Communications* 2016 7:1. 7 (2016) 1–13. 10.1038/ncomms13193.
- [70]. Umeki Y, Mohri K, Kawasaki Y, Watanabe H, Takahashi R, Takahashi Y, Takakura Y, Nishikawa M, Induction of Potent Antitumor Immunity by Sustained Release of Cationic Antigen from a DNA-Based Hydrogel with Adjuvant Activity, *Advanced Functional Materials*. 25 (2015) 5758–5767. 10.1002/ADFM.201502139.
- [71]. Lynn GM, Laga R, Darrah PA, Ishizuka AS, Balaci AJ, Dulcey AE, Pechar M, Pola, Gerner MY, Yamamoto A, Buechler CR, Quinn KM, Smelkinson MG, Vanek O, Cawood R, Hills, Vasalatiy O, Kastenmüller K, Francica JR, Stutts, Tom JK, Ryu KA, Esser-Kahn AP, Etrych, Fisher KD, Seymour LW, Seder RA, In vivo characterization of the physicochemical properties of

- polymer-linked TLR agonists that enhance vaccine immunogenicity, *Nat Biotechnol.* 33 (2015) 1201–1210. 10.1038/NBT.3371. [PubMed: 26501954]
- [72]. Dubrot J, Portero A, Orive G, Hernández RM, Palazón A, Rouzaut A, Perez-Gracia JL, Hervás-Stubbs S, Pedraz JL, Melero I, Delivery of immunostimulatory monoclonal antibodies by encapsulated hybridoma cells, *Cancer Immunology, Immunotherapy* 2010 59:11. 59 (2010) 1621–1631. 10.1007/S00262-010-0888-Z.
- [73]. Kim J, Li WA, Choi Y, Lewin SA, Verbeke CS, Dranoff G, Mooney DJ, Injectable, spontaneously assembling, inorganic scaffolds modulate immune cells in vivo and increase vaccine efficacy, *Nature Biotechnology* 2014 33:1. 33 (2014) 64–72. 10.1038/nbt.3071.
- [74]. Q W, MT T, BP K, MA B, MJ H, Time course study of the antigen-specific immune response to a PLGA microparticle vaccine formulation, *Biomaterials.* 35 (2014) 8385–8393. 10.1016/J.BIOMATERIALS.2014.05.067. [PubMed: 24986256]
- [75]. Kuai R, Ochyl LJ, Bahjat KS, Schwendeman A, Moon JJ, Designer vaccine nanodiscs for personalized cancer immunotherapy, *Nature Materials* 2017 16:4. 16 (2016) 489–496. 10.1038/nmat4822.
- [76]. Pan Y, Li X, Kang T, Meng H, Chen Z, Yang L, Wu Y, Wei Y, Gou M, Efficient delivery of antigen to DCs using yeast-derived microparticles, *Sci Rep.* 5 (2015). 10.1038/SREP10687.
- [77]. Song H, Huang P, Niu J, Shi G, Zhang C, Kong D, Wang W, Injectable polypeptide hydrogel for dual-delivery of antigen and TLR3 agonist to modulate dendritic cells in vivo and enhance potent cytotoxic T-lymphocyte response against melanoma, *Biomaterials.* 159 (2018) 119–129. 10.1016/J.BIOMATERIALS.2018.01.004. [PubMed: 29324304]
- [78]. Li AW, Sobral MC, Badrinath S, Choi Y, Graveline A, Stafford AG, Weaver JC, Dellacherie MO, Shih T-Y, Ali OA, Kim J, Wucherpfennig KW, Mooney DJ, A facile approach to enhance antigen response for personalized cancer vaccination, *Nature Materials* 2018 17:6. 17 (2018) 528–534. 10.1038/s41563-018-0028-2.
- [79]. Wang C, Sun W, Wright G, Wang AZ, Gu Z, Inflammation-Triggered Cancer Immunotherapy by Programmed Delivery of CpG and Anti-PD1 Antibody, *Adv Mater.* 28 (2016) 8912–8920. 10.1002/ADMA.201506312. [PubMed: 27558441]
- [80]. Sippel S, Muruganandan K, Levine A, Shah S, Review article: Use of ultrasound in the developing world, *International Journal of Emergency Medicine* 2011 4:1. 4 (2011) 1–11. 10.1186/1865-1380-4-72.
- [81]. Computer tomography scanners density by country 2019, Statista. (2019). <https://www.statista.com/statistics/266539/distribution-of-equipment-for-computer-tomography/> (accessed October 24, 2021).
- [82]. Kanmounye US, Zolo Y, Robertson FC, Bankole NDA, Kabulo KDM, Ntalaja JM, Magogo J, Negida A, Thango N, Esene I, Pennicooke B, Molina CA, Prevalence of spine surgery navigation techniques and availability in Africa: A cross-sectional study, *Annals of Medicine and Surgery.* 68 (2021) 102637. 10.1016/J.AMSU.2021.102637. [PubMed: 34386229]
- [83]. Wang D, Image Guidance Technologies for Interventional Pain Procedures: Ultrasound, Fluoroscopy, and CT, *Current Pain and Headache Reports.* 22 (2018). 10.1007/s11916-018-0660-1.
- [84]. Yang G, Liu J, Ma L, Cai Z, Meng C, Qi S, Zhou H, Ultrasound-guided versus fluoroscopy-controlled lumbar transforaminal epidural injections: A prospective randomized clinical trial, *Clinical Journal of Pain.* 32 (2016) 103–108. 10.1097/AJP.000000000000237. [PubMed: 25803759]
- [85]. Kosaka N, Ogawa M, Choyke PL, Kobayashi H, Clinical implications of near-infrared fluorescence imaging in cancer, 10.2217/Fon.09.109. 5 (2009) 1501–1511. 10.2217/FON.09.109.
- [86]. Zhu B, Sevick-Muraca EM, A review of performance of near-infrared fluorescence imaging devices used in clinical studies, 10.1259/Bjr.20140547. 88 (2014). 10.1259/BJR.20140547.
- [87]. de Bournonville S, Vangrunderbeeck S, Kerckhofs G, Contrast-enhanced microCT for virtual 3D anatomical pathology of biological tissues: A literature review, *Contrast Media and Molecular Imaging.* 2019 (2019). 10.1155/2019/8617406.



- [88]. Lewis JS, Achilefu S, Garbow JR, Laforest R, Welch MJ, Small animal imaging: current technology and perspectives for oncological imaging, *European Journal of Cancer*. 38 (2002) 2173–2188. 10.1016/S0959-8049(02)00394-5. [PubMed: 12387842]
- [89]. Mirniaharikandehei S, VanOsdol J, Heidari M, Danala G, Sethuraman SN, Ranjan A, Zheng B, Developing a Quantitative Ultrasound Image Feature Analysis Scheme to Assess Tumor Treatment Efficacy Using a Mouse Model, *Scientific Reports* 2019 9:1. 9 (2019) 1–10. 10.1038/s41598-019-43847-7.
- [90]. Correa S, Grosskopf AK, Lopez Hernandez H, Chan D, Yu AC, Stapleton LM, Appel EA, Translational Applications of Hydrogels, *Chemical Reviews*. 121 (2021) 11385–11457. 10.1021/ACS.CHEMREV.0C01177. [PubMed: 33938724]
- [91]. Sudhyadhom A, On the molecular relationship between Hounsfield Unit (HU), mass density, and electron density in computed tomography (CT), *PLOS ONE*. 15 (2020) e0244861. 10.1371/JOURNAL.PONE.0244861. [PubMed: 33382794]
- [92]. Sheth S, Scatarige JC, Horton KM, Corl FM, Fishman EK, Current Concepts in the Diagnosis and Management of Renal Cell Carcinoma: Role of Multidetector CT and Three-dimensional CT1, *10.1148/Radiographics.21.Suppl\_1.G01oc18s237*. 21 (2001). 10.1148/RADIOGRAPHICS.21.SUPPL\_1.G01OC18S237.
- [93]. Cosgrove D, Ultrasound contrast agents: An overview, *European Journal of Radiology*. 60 (2006) 324–330. 10.1016/J.EJRAD.2006.06.022. [PubMed: 16938418]
- [94]. Appelbaum L, Kane RA, Kruskal JB, Romero J, Sosna J, Focal Hepatic Lesions: US-guided Biopsy—Lessons from Review of Cytologic and Pathologic Examination Results, *10.1148/Radiol.2502080182*. 250 (2009) 453–458. 10.1148/RADIOL.2502080182.
- [95]. Mishra A, Tarsin R, Elhabbash B, Zagan N, Markus R, Drebecka S, Abdelmola K, Shawish T, Shebani A, Abdelmola T, Elusta A, Ehtuish EF, Percutaneous ultrasound-guided renal biopsy., *Saudi J Kidney Dis Transpl*. 22 (2011) 746–750. [PubMed: 21743221]
- [96]. M M, A A, O M, Ultrasound- Versus CT-Guided Subpleural Lung and Pleural Biopsy: An Analysis of Wait Times, Procedure Time, Safety, and Diagnostic Adequacy, *Can Assoc Radiol J*. 72 (2021) 883–889. 10.1177/0846537120939073. [PubMed: 32673070]
- [97]. Wang G, Snyder DL, O’Sullivan JA, Vannier MW, Iterative deblurring for CT metal artifact reduction, *IEEE Transactions on Medical Imaging*. 15 (1996) 657–664. 10.1109/42.538943. [PubMed: 18215947]
- [98]. de Crop A, Casselman J, van Hoof T, Dierens M, Vereecke E, Bossu N, Pamplona J, D’Herde K, Thierens H, Bacher K, Analysis of metal artifact reduction tools for dental hardware in CT scans of the oral cavity: kVp, iterative reconstruction, dual-energy CT, metal artifact reduction software: does it make a difference?, *Neuroradiology* 2015 57:8. 57 (2015) 841–849. 10.1007/S00234-015-1537-1.
- [99]. Saini A, Wallace A, Alzubaidi S, Knuttinen MG, Naidu S, Sheth R, Albadawi H, Oklu R, History and Evolution of Yttrium-90 Radioembolization for Hepatocellular Carcinoma, *Journal of Clinical Medicine* 2019, Vol. 8, Page 55. 8 (2019) 55. 10.3390/JCM8010055.
- [100]. Vogl TJ, Zangos S, Balzer JO, Nabil M, Rao P, Eichler K, Bechstein WO, Zeuzem S, Abdelkader A, Transarterial chemoembolization (TACE) in hepatocellular carcinoma: technique, indication and results., *Rofo : Fortschritte Auf Dem Gebiete Der Rontgenstrahlen Und Der Nuklearmedizin*. 179 (2007) 1113–1126. 10.1055/S-2007-963285. [PubMed: 17948190]
- [101]. LC Bead LUMI™ - Boston Scientific, (n.d.). <https://www.bostonscientific.com/en-US/products/embolization/lc-bead-lumi.html> (accessed November 3, 2021).
- [102]. Aliberti C, Carandina R, Sarti D, Pizzirani E, Ramondo G, Cillo U, Guadagni S, Fiorentini G, Transarterial chemoembolization with DC Bead LUMITM radiopaque beads for primary liver cancer treatment: Preliminary experience, *Future Oncology*. 13 (2017) 2243–2252. 10.2217/FON-2017-0364/ASSET/IMAGES/LARGE/FIGURE5.JPEG. [PubMed: 29063780]
- [103]. Arepally A, Targeted drug delivery under MRI guidance, *Journal of Magnetic Resonance Imaging*. 27 (2008) 292–298. 10.1002/jmri.21266. [PubMed: 18219683]
- [104]. Fernando R, Downs J, Maples D, Ranjan A, MRI-guided monitoring of thermal dose and targeted drug delivery for cancer Therapy, *Pharmaceutical Research*. 30 (2013) 2709–2717. 10.1007/s11095-013-1110-8. [PubMed: 23780716]



- [105]. Napoli A, Anzidei M, de Nunzio C, Cartocci G, Panebianco V, de Dominicis C, Catalano C, Petrucci F, Leonardo C, Real-time Magnetic Resonance-guided High-intensity Focused Ultrasound Focal Therapy for Localised Prostate Cancer: Preliminary Experience, *European Urology*. 63 (2013) 395–398. 10.1016/J.EURURO.2012.11.002. [PubMed: 23159454]
- [106]. Klaeser B, Mueller MD, Schmid RA, Guevara C, Krause T, Wiskirchen J, PET-CT-guided interventions in the management of FDG-positive lesions in patients suffering from solid malignancies: initial experiences, *European Radiology* 2009 19:7. 19 (2009) 1780–1785. 10.1007/S00330-009-1338-1.
- [107]. Rajagopal M, Venkatesan AM, Image fusion and navigation platforms for percutaneous image-guided interventions, *Abdominal Radiology* 2016 41:4. 41 (2016) 620–628. 10.1007/S00261-016-0645-7.
- [108]. Govindarajan M, Nagaraj K, Kallur K, Sridhar P, PET/CT guidance for percutaneous fine needle aspiration cytology/biopsy, *The Indian Journal of Radiology & Imaging*. 19 (2009) 208. 10.4103/0971-3026.54885.
- [109]. Sheth RA, Arellano RS, Uppot RN, Samir AE, Goyal L, Zhu AX, Gervais DA, Mahmood U, Prospective trial with optical molecular imaging for percutaneous interventions in focal hepatic lesions, *Radiology*. 274 (2015) 917–926. 10.1148/RADIOL.14141308/ASSET/IMAGES/LARGE/RADIOL.14141308.FIG7.JPEG. [PubMed: 25302707]
- [110]. Solomon R, Contrast media: Are there differences in nephrotoxicity among contrast media?, *BioMed Research International*. 2014 (2014). 10.1155/2014/934947.
- [111]. Miyamoto Y, Tsujimoto T, Iwai K, Ishida K, Uchimoto R, Miyazawa T, Azuma H, Safety and pharmacokinetics of iotrolan in hysterosalpingography. Retention and irritability compared with Lipiodol, *Invest Radiol*. 30 (1995) 538–543. 10.1097/00004424-199509000-00005. [PubMed: 8537211]
- [112]. Omata D, Unga J, Suzuki R, Maruyama K, Lipid-based microbubbles and ultrasound for therapeutic application, *Advanced Drug Delivery Reviews*. 154–155 (2020) 236–244. 10.1016/J.ADDR.2020.07.005.
- [113]. Chertok B, Langer R, Circulating Magnetic Microbubbles for Localized Real-Time Control of Drug Delivery by Ultrasonography-Guided Magnetic Targeting and Ultrasound, 8 (2018). 10.7150/thno.20781.
- [114]. Dong YC, Bouché M, Uman S, Burdick JA, Cormode DP, Detecting and Monitoring Hydrogels with Medical Imaging, *ACS Biomaterials Science & Engineering*. 7 (2021) 4027–4047. 10.1021/ACSBIOMATERIALS.0C01547. [PubMed: 33979137]
- [115]. Sun Z, Song C, Wang C, Hu Y, Wu J, Hydrogel-Based Controlled Drug Delivery for Cancer Treatment: A Review, *Molecular Pharmaceutics*. 17 (2019) 373–391. 10.1021/ACS.MOLPHARMACEUT.9B01020.
- [116]. Han X, Huang J, To AKW, Lai JHC, Xiao P, Wu EX, Xu J, Chan KWY, CEST MRI detectable liposomal hydrogels for multiparametric monitoring in the brain at 3T, *Theranostics*. 10 (2020) 2215–2228. 10.7150/THNO.40146. [PubMed: 32089739]
- [117]. Zhu W, Chu C, Kuddannaya S, Yuan Y, Walczak P, Singh A, Song X, Bulte JWM, In Vivo Imaging of Composite Hydrogel Scaffold Degradation Using CEST MRI and Two-Color NIR Imaging, *Adv Funct Mater*. 29 (2019). 10.1002/ADFM.201903753.
- [118]. Lock LL, Li Y, Mao X, Chen H, Staedtke V, Bai R, Ma W, Lin R, Li Y, Liu G, Cui H, One-Component Supramolecular Filament Hydrogels as Theranostic Label-Free Magnetic Resonance Imaging Agents, *ACS Nano*. 11 (2017) 797. 10.1021/ACS.NANO.6B07196. [PubMed: 28075559]
- [119]. Xu H-X, Tan Y, Wang D, Wang X-L, An W-L, Xu P-P, Xu S, Wang Y-Z, Autofluorescence of hydrogels without a fluorophore, *Soft Matter*. 15 (2019) 3588–3594. 10.1039/C9SM00034H. [PubMed: 30964145]
- [120]. Ma X, Sun X, Hargrove D, Chen J, Song D, Dong Q, Lu X, Fan TH, Fu Y, Lei Y, A Biocompatible and Biodegradable Protein Hydrogel with Green and Red Autofluorescence: Preparation, Characterization and In Vivo Biodegradation Tracking and Modeling, *Sci Rep*. 6 (2016). 10.1038/SREP19370.

- [121]. Jin R, Yang X, Zhao D, Hou X, Li C, Song X, Chen W, Wang Q, Zhao Y, Liu B, An injectable hybrid hydrogel based on a genetically engineered polypeptide for second near-infrared fluorescence/photoacoustic imaging-monitored sustained chemo-photothermal therapy, *Nanoscale*. 11 (2019) 16080–16091. 10.1039/C9NR04630E. [PubMed: 31432846]
- [122]. Wang L, Li B, Xu F, Li Y, Xu Z, Wei D, Feng Y, Wang Y, Jia D, Zhou Y, Visual in vivo degradation of injectable hydrogel by real-time and non-invasive tracking using carbon nanodots as fluorescent indicator, *Biomaterials*. 145 (2017) 192–206. 10.1016/J.BIOMATERIALS.2017.08.039. [PubMed: 28869865]
- [123]. Fan D, Fei X, Tian J, Zhi H, Xu L, Wang X, Wang Y, Synthesis and investigation of a novel luminous hydrogel, *Polymer Chemistry*. 7 (2016) 3766–3772. 10.1039/C6PY00749J.
- [124]. Jin H, Zhao G, Hu J, Ren Q, Yang K, Wan C, Huang A, Li P, JP. Feng, J. Chen, Z. Zou, Melittin-Containing Hybrid Peptide Hydrogels for Enhanced Photothermal Therapy of Glioblastoma, *ACS Appl Mater Interfaces*. 9 (2017) 25755–25766. 10.1021/ACSAMI.7B06431. [PubMed: 28714303]
- [125]. Kim JH, Lim SY, Nam DH, Ryu J, Ku SH, Park CB, Self-assembled, photoluminescent peptide hydrogel as a versatile platform for enzyme-based optical biosensors, *Biosens Bioelectron*. 26 (2011) 1860–1865. 10.1016/J.BIOS.2010.01.026. [PubMed: 20171868]
- [126]. Chen X, Zhang J, Wu K, Wu X, Tang J, Cui S, Cao D, Liu R, Peng C, Yu L, Ding J, Visualizing the In Vivo Evolution of an Injectable and Thermosensitive Hydrogel Using Tri-Modal Bioimaging, *Small Methods*. 4 (2020) 2000310. 10.1002/SMTD.202000310.
- [127]. Lee D, Heo DN, Nah HR, Lee SJ, Ko W-K, Lee JS, Moon H-J, Bang JB, Hwang Y-S, Reis RL, Kwon IK, Injectable hydrogel composite containing modified gold nanoparticles: implication in bone tissue regeneration, *International Journal of Nanomedicine*. 13 (2018) 7019. 10.2147/IJN.S185715. [PubMed: 30464456]
- [128]. Wu Y, Wang H, Gao F, Xu Z, Dai F, Liu W, An Injectable Supramolecular Polymer Nanocomposite Hydrogel for Prevention of Breast Cancer Recurrence with Theranostic and Mammoplastic Functions, *Advanced Functional Materials*. 28 (2018) 1801000. 10.1002/ADFM.201801000.
- [129]. Wu X, Wang X, Chen X, Yang X, Ma Q, Xu G, Yu L, Ding J, Injectable and thermosensitive hydrogels mediating a universal macromolecular contrast agent with radiopacity for noninvasive imaging of deep tissues, *Bioactive Materials*. 6 (2021) 4717–4728. 10.1016/J.BIOACTMAT.2021.05.013. [PubMed: 34136722]
- [130]. Coutu JM, Fatimi A, Berrahmoune S, Soulez G, Lerouge S, A new radiopaque embolizing agent for the treatment of endoleaks after endovascular repair: influence of contrast agent on chitosan thermogel properties, *J Biomed Mater Res B Appl Biomater*. 101 (2013) 153–161. 10.1002/JBM.B.32828. [PubMed: 23090727]
- [131]. Barnett BP, Hughes AH, Lin S, Arepally A, Gailloud PH, In vitro assessment of EmboGel and UltraGel radiopaque hydrogels for the endovascular treatment of aneurysms, *J Vasc Interv Radiol*. 20 (2009) 507–512. 10.1016/J.JVIR.2009.01.005. [PubMed: 19328428]
- [132]. Leng X, Liu B, Su B, Liang M, Shi L, Li S, Qu S, Fu X, Liu Y, Yao M, Kaplan DL, Wang Y, Wang X, In situ ultrasound imaging of silk hydrogel degradation and neovascularization, *J Tissue Eng Regen Med*. 11 (2017) 822–830. 10.1002/TERM.1981. [PubMed: 25850825]
- [133]. Larkin J, Chiarion-Sileni V, Gonzalez R, Grob JJ, Cowey CL, Lao CD, Schadendorf D, Dummer R, Smylie M, Rutkowski P, Ferrucci PF, Hill A, Wagstaff J, Carlino MS, Haanen JB, Maio M, Marquez-Rodas I, McArthur GA, Ascierto PA, Long G. v, Callahan MK, Postow MA, Grossmann K, Sznol M, Dreno B, Bastholt L, Yang A, Rollin LM, Horak C, Hodi FS, Wolchok JD, Combined Nivolumab and Ipilimumab or Monotherapy in Untreated Melanoma, *New England Journal of Medicine*. 373 (2015) 23–34. 10.1056/nejmoa1504030. [PubMed: 26027431]
- [134]. Motzer RJ, Escudier B, McDermott DF, George S, Hammers HJ, Srinivas S, Tykodi SS, Sosman JA, Procopio G, Plimack ER, Castellano D, Choueiri TK, Gurney H, Donskov F, Bono, Wagstaff J, Gauder TC, Ueda T, Tomita Y, Schutz FA, Kollmannsberger C, Larkin J, Ravaud A, Simon JS, Xu LA, Waxman IM, Sharma P, Nivolumab versus Everolimus in Advanced Renal-Cell Carcinoma, *N Engl J Med*. 373 (2015) 1803–1813. 10.1056/NEJMoa1510665. [PubMed: 26406148]

- [135]. Ansell SM, Lesokhin AM, Borrello I, Halwani A, Scott EC, Gutierrez M, Schuster SJ, Millenson MM, Cattray D, Freeman GJ, Rodig SJ, Chapuy B, Ligon AH, Zhu L, Grosso JF, Kim SY, Timmerman JM, Shipp MA, Armand P, PD-1 Blockade with Nivolumab in Relapsed or Refractory Hodgkin's Lymphoma, *New England Journal of Medicine*. 372 (2015) 311–319. 10.1056/nejmoa1411087. [PubMed: 25482239]
- [136]. Ferris RL, Blumenschein G, Fayette J, Guigay J, Colevas AD, Licitra L, Harrington K, Kasper S, Vokes EE, Even C, Worden F, Saba NF, Iglesias Docampo LC, Haddad R, Rordorf T, Kiyota N, Tahara M, Monga M, Lynch M, Geese WJ, Kopit J, Shaw JW, Gillison ML, Nivolumab for Recurrent Squamous-Cell Carcinoma of the Head and Neck, *New England Journal of Medicine*. 375 (2016) 1856–1867. 10.1056/nejmoa1602252. [PubMed: 27718784]
- [137]. Borghaei H, Paz-Ares L, Horn L, Spigel DR, Steins M, Ready NE, Chow LQ, Vokes EE, Felip E, Holgado E, Barlesi F, Kohlhäufel M, Arrieta O, Burgio MA, Fayette J, Lena H, Poddubskaya E, Gerber DE, Gettinger SN, Rudin CM, Rizvi N, Crinò L, Blumenschein GR, Antonia SJ, Dorange C, Harbison CT, Graf Finckenstein F, Brahmer JR, Nivolumab versus Docetaxel in Advanced Nonsquamous Non–Small-Cell Lung Cancer, *New England Journal of Medicine*. 373 (2015) 1627–1639. 10.1056/nejmoa1507643. [PubMed: 26412456]
- [138]. Hamanishi J, Mandai M, Ikeda T, Minami M, Kawaguchi A, Murayama T, Kanai M, Mori Y, Matsumoto S, Chikuma S, Matsumura N, Abiko K, Baba T, Yamaguchi K, Ueda A, Hosoe Y, Morita S, Yokode M, Shimizu A, Honjo T, Konishi I, Safety and antitumor activity of Anti-PD-1 antibody, nivolumab, in patients with platinum-resistant ovarian cancer, *Journal of Clinical Oncology*. 33 (2015) 4015–4022. 10.1200/JCO.2015.62.3397. [PubMed: 26351349]
- [139]. Robert C, Schachter J, Long G. v, Arance, Grob JJ, Mortier L, Daud A, Carlino MS, McNeil, Lotem M, Larkin J, Lorigan P, Neyns B, Blank CU, Hamid O, Mateus C, Shapira-Frommer R, Kosh M, Zhou H, Ibrahim N, Ebbinghaus S, Ribas A, Pembrolizumab versus Ipilimumab in Advanced Melanoma, *New England Journal of Medicine*. 372 (2015) 2521–2532. 10.1056/nejmoa1503093. [PubMed: 25891173]
- [140]. Nghiem PT, Bhatia S, Lipson EJ, Kudchadkar RR, Miller NJ, Annamalai L, Berry S, Chartash EK, Daud A, Fling SP, Friedlander PA, Kluger HM, Kohrt HE, Lundgren L, Margolin K, Mitchell A, Olencki T, Pardoll DM, Reddy SA, Shantha EM, Sharfman WH, Sharon E, Shemanski LR, Shinohara MM, Sunshine JC, Taube JM, Thompson JA, Townson SM, Yearley JH, Topalian SL, Cheever MA, PD-1 Blockade with Pembrolizumab in Advanced Merkel-Cell Carcinoma, *New England Journal of Medicine*. 374 (2016) 2542–2552. 10.1056/nejmoa1603702. [PubMed: 27093365]
- [141]. Garon EB, Rizvi NA, Hui R, Leigh N, Balmanoukian AS, Eder JP, Patnaik A, Aggarwal C, Gubens M, Horn L, Carcereny E, Ahn M-J, Felip E, Lee J-S, Hellmann MD, Hamid O, Goldman JW, Soria J-C, Dolled-Filhart M, Rutledge RZ, Zhang J, Luceford JK, Rangwala R, Lubiniecki GM, Roach C, Emancipator K, Gandhi L, Pembrolizumab for the Treatment of Non–Small-Cell Lung Cancer, *New England Journal of Medicine*. 372 (2015) 2018–2028. 10.1056/nejmoa1501824. [PubMed: 25891174]
- [142]. Le DT, Uram JN, Wang H, Bartlett BR, Kemberling H, Eyring AD, Skora AD, Luber BS, Azad NS, Laheru D, Biedrzycki B, Donehower RC, Zaheer A, Fisher GA, Crocenzi TS, Lee JJ, Duffy SM, Goldberg RM, de la Chapelle A, Koshiji M, Bhaijee F, Huebner T, Hruban RH, Wood LD, Cuka N, Pardoll DM, Papadopoulos N, Kinzler KW, Zhou S, Cornish TC, Taube JM, Anders RA, Eshleman JR, Vogelstein B, Diaz LA, PD-1 Blockade in Tumors with Mismatch-Repair Deficiency, *New England Journal of Medicine*. 372 (2015) 2509–2520. 10.1056/nejmoa1500596. [PubMed: 26028255]
- [143]. Armand P, Nagler A, Weller EA, Devine SM, Avigan DE, bin Chen Y, Kaminski MS, Holland HK, Winter JN, Mason JR, Fay JW, Rizzieri DA, Hosing CM, Ball ED, Uberti JP, Lazarus HM, Mapara MY, Gregory SA, Timmerman JM, Andorsky D, Or R, Waller EK, Rotem-Yehudar R, Gordon LI, Disabling immune tolerance by programmed death-1 blockade with pidilizumab after autologous hematopoietic stem-cell transplantation for diffuse large B-cell lymphoma: results of an international phase II trial, *J Clin Oncol*. 31 (2013) 4199–4206. 10.1200/JCO.2012.48.3685. [PubMed: 24127452]
- [144]. Westin JR, Chu F, Zhang M, Fayad LE, Kwak LW, Fowler N, Romaguera J, Hagemester F, Fanale M, Samaniego F, Feng L, Baladandayuthapani V, Wang Z, Ma W, Gao Y, Wallace M, Vence LM, Radvanyi L, Muzzafar T, Rotem-Yehudar R, Davis RE, Neelapu SS, Safety and

activity of PD1 blockade by pidilizumab in combination with rituximab in patients with relapsed follicular lymphoma: A single group, open-label, phase 2 trial, *The Lancet Oncology*. 15 (2014) 69–77. 10.1016/S1470-2045(13)70551-5. [PubMed: 24332512]

- [145]. Robert C, Thomas L, Bondarenko I, O'Day S, Weber J, Garbe C, Lebbe C, Baurain J-F, Testori A, Grob J-J, Davidson N, Richards J, Maio M, Hauschild A, Miller WH, Gascon P, Lotem M, Harmankaya K, Ibrahim R, Francis S, Chen T-T, Humphrey R, Hoos A, Wolchok JD, Ipilimumab plus Dacarbazine for Previously Untreated Metastatic Melanoma, *New England Journal of Medicine*. 364 (2011) 2517–2526. 10.1056/nejmoa1104621. [PubMed: 21639810]
- [146]. Ribas A, Kefford R, Marshall MA, Punt CJA, Haanen JB, Marmol M, Garbe C, Gogas H, Schachter J, Linette G, Lorigan P, Kendra KL, Maio M, Trefzer U, Smylie M, McArthur GA, Dreno B, Nathan PD, MacKiewicz J, Kirkwood JM, Gomez-Navarro J, Huang B, Pavlov D, Hauschild A, Phase III randomized clinical trial comparing tremelimumab with standard-of-care chemotherapy in patients with advanced melanoma, *Journal of Clinical Oncology*. 31 (2013) 616–622. 10.1200/JCO.2012.44.6112. [PubMed: 23295794]
- [147]. Antonia SJ, López-Martin JA, Bendell J, Ott PA, Taylor M, Eder JP, Jäger D, Pietanza MC, Le DT, de Braud F, Morse MA, Ascierto PA, Horn L, Amin A, Pillai RN, Evans J, Chau I, Bono P, Atmaca A, Sharma P, Harbison CT, Lin CS, Christensen O, Calvo E, Nivolumab alone and nivolumab plus ipilimumab in recurrent small-cell lung cancer (CheckMate 032): a multicentre, open-label, phase 1/2 trial, *The Lancet Oncology*. 17 (2016) 883–895. 10.1016/S1470-2045(16)30098-5. [PubMed: 27269741]
- [148]. Zhu M, Ding X, Zhao R, Liu X, Shen H, Cai C, Ferrari M, Wang HY, Wang R-F, Co-delivery of tumor antigen and dual toll-like receptor ligands into dendritic cell by silicon microparticle enables efficient immunotherapy against melanoma, *J Control Release*. 272 (2018) 72. 10.1016/J.JCONREL.2018.01.004. [PubMed: 29325699]
- [149]. Keshavarz M, Moloudi K, Paydar R, Abed Z, Beik J, Ghaznavi H, Shakeri-Zadeh A, Alginate hydrogel co-loaded with cisplatin and gold nanoparticles for computed tomography image-guided chemotherapy., *Journal of Biomaterials Applications*. 33 (2018) 161–169. 10.1177/0885328218782355. [PubMed: 29933708]
- [150]. Hong S, Carlson J, Lee H, Weissleder R, Bioorthogonal Radiopaque Hydrogel for Endoscopic Delivery and Universal Tissue Marking, *Adv Healthc Mater*. 5 (2016) 421–426. 10.1002/ADHM.201500780. [PubMed: 26688173]
- [151]. Bouché M, Dong YC, Sheikh S, Taing K, Saxena D, Hsu JC, Chen MH, Salinas RD, Song H, Burdick JA, Dorsey J, Cormode DP, Novel treatment for glioblastoma delivered by a radiation responsive and radiopaque hydrogel, *ACS Biomaterials Science and Engineering*. 7 (2021) 3209–3220. 10.1021/ACSBIOMATERIALS.1C00385. [PubMed: 34160196]
- [152]. Zhang Y, Gao H, Wang H, Xu Z, Chen X, Liu B, Shi Y, Lu Y, Wen L, Li Z, Men Y, Feng X, Liu W, Radiopaque Highly Stiff and Tough Shape Memory Hydrogel Microcoils for Permanent Embolization of Arteries, *Advanced Functional Materials*. 28 (2018) 1705962. 10.1002/ADFM.201705962.
- [153]. Lei K, Chen Y, Wang J, Peng X, Yu L, Ding J, Non-invasive monitoring of in vivo degradation of a radiopaque thermoreversible hydrogel and its efficacy in preventing post-operative adhesions, *Acta Biomaterialia*. 55 (2017) 396–409. 10.1016/J.ACTBIO.2017.03.042. [PubMed: 28363786]
- [154]. Hong S, Carlson J, Lee H, Weissleder R, Bioorthogonal radiopaque hydrogel for endoscopic delivery and universal tissue marking, *Adv Healthc Mater*. 5 (2016) 421. 10.1002/ADHM.201500780. [PubMed: 26688173]
- [155]. Jin H, Zhao G, Hu J, Ren Q, Yang K, Wan C, Huang A, Li P, Feng JP, Chen J, Zou Z, Melittin-Containing Hybrid Peptide Hydrogels for Enhanced Photothermal Therapy of Glioblastoma, *ACS Appl Mater Interfaces*. 9 (2017) 25755–25766. 10.1021/ACSAMI.7B06431. [PubMed: 28714303]
- [156]. Kim JI, Lee BS, Chun C, Cho JK, Kim SY, Song SC, Long-term theranostic hydrogel system for solid tumors, *Biomaterials*. 33 (2012) 2251–2259. 10.1016/J.BIOMATERIALS.2011.11.083. [PubMed: 22189146]
- [157]. Bakker MH, Tseng CCS, Keizer HM, Seevinck PR, Janssen HM, van Slochteren FJ, Chamuleau SAJ, Dankers PYW, MRI Visualization of Injectable Ureidopyrimidinone Hydrogelators by

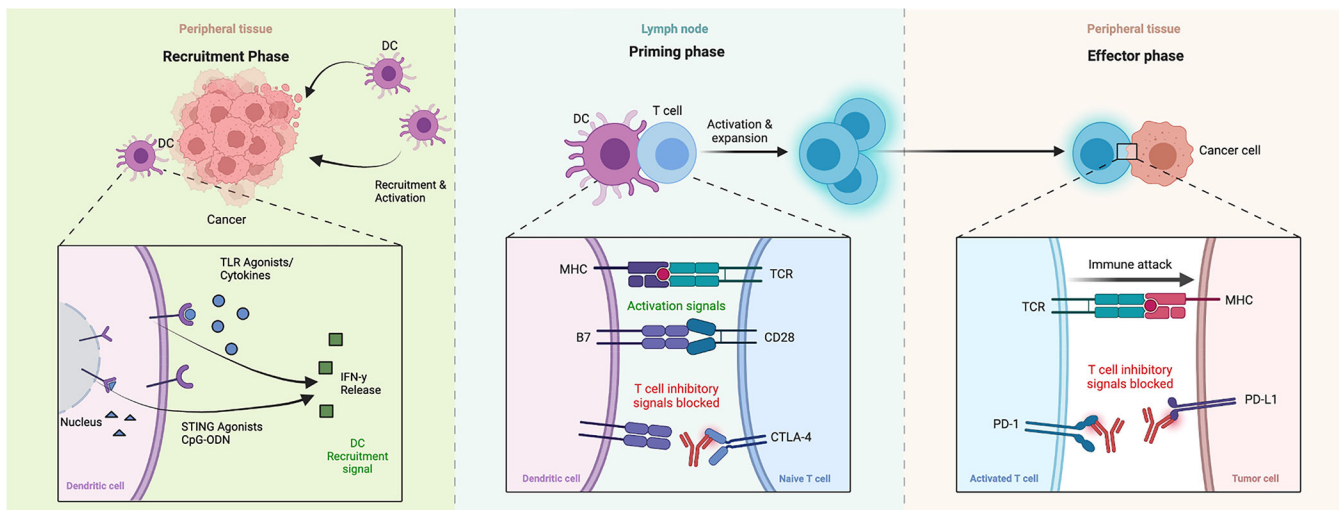
Supramolecular Contrast Agent Labeling, *Advanced Healthcare Materials*. 7 (2018). 10.1002/ADHM.201701139.

- [158]. Chen B, Xing J, Li M, Liu Y, Ji M, DOX@Ferumoxytol-Medical Chitosan as magnetic hydrogel therapeutic system for effective magnetic hyperthermia and chemotherapy in vitro, *Colloids Surf B Biointerfaces*. 190 (2020). 10.1016/J.COLSURFB.2020.110896.
- [159]. Patrick PS, Bear JC, Fitzke HE, Zaw-Thin M, Parkin IP, Lythgoe MF, Kalber TL, Stuckey DJ, Radio-metal cross-linking of alginate hydrogels for non-invasive in vivo imaging, *Biomaterials*. 243 (2020). 10.1016/J.BIOMATERIALS.2020.119930.
- [160]. Laurén P, Lou YR, Raki M, Urtti A, Bergström K, Yliperttula M, Technetium-99m-labeled nanofibrillar cellulose hydrogel for in vivo drug release, *European Journal of Pharmaceutical Sciences*. 65 (2014) 79–88. 10.1016/J.EJPS.2014.09.013. [PubMed: 25245005]
- [161]. Kopf H, Mostbeck GH, Loizides A, Gruber H, Ultrasound-guided interventions at peripheral nerves: Diagnostic and therapeutic indications, *Ultraschall in Der Medizin*. 32 (2011) 440–459. 10.1055/S-0031-1281762. [PubMed: 21986925]

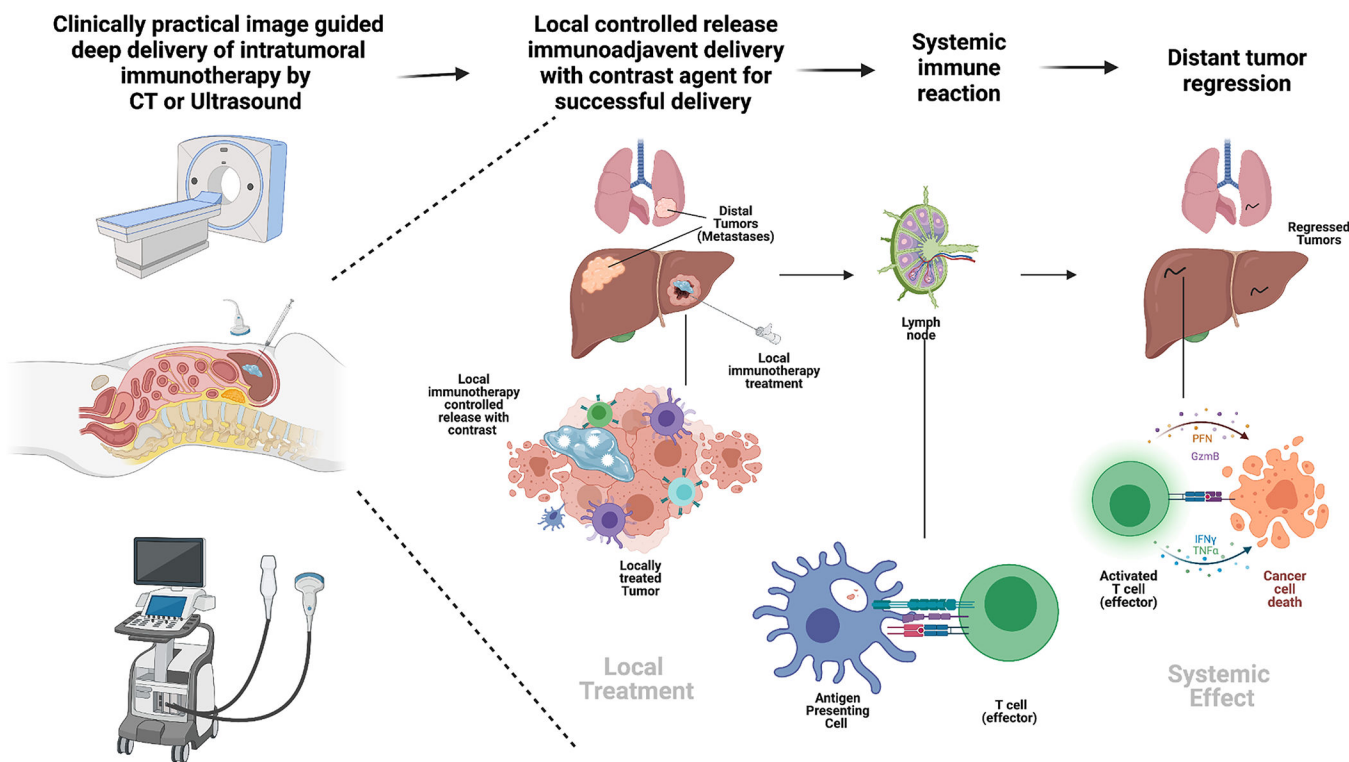
### Highlights

- Intratumoral immunotherapy is a rapidly growing clinical field bridging clinical image guided delivery by interventional radiology and controlled release drug delivery.
- Real-time imaging feedback is necessary to ensure proper intratumoral delivery.
- A variety of imaging modalities are under scientific exploration, yet only a few have the potential for near-future application in clinical settings, particularly CT and ultrasound.
- Eventual clearance of the imaging contrast agent is ideal to minimize impact on interpretation of subsequent staging studies.
- Controlled-release formulations will improve clinical adoption by minimizing the need for multiple procedures and may enhance efficacy of intratumoral immunoadjuvants.

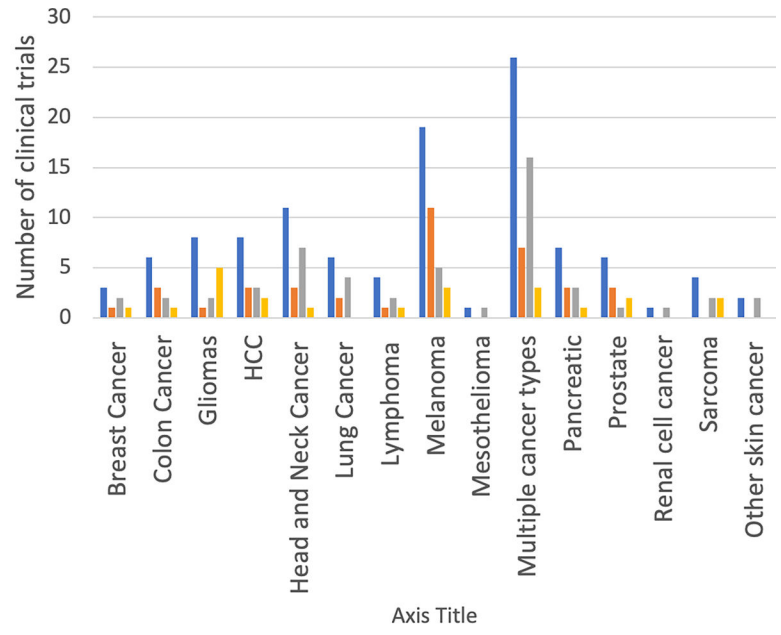
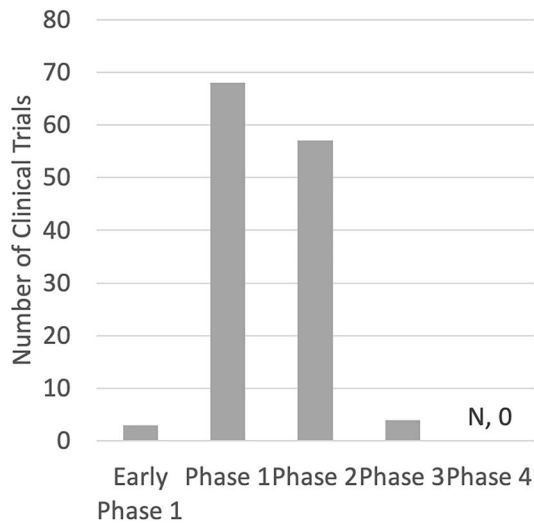




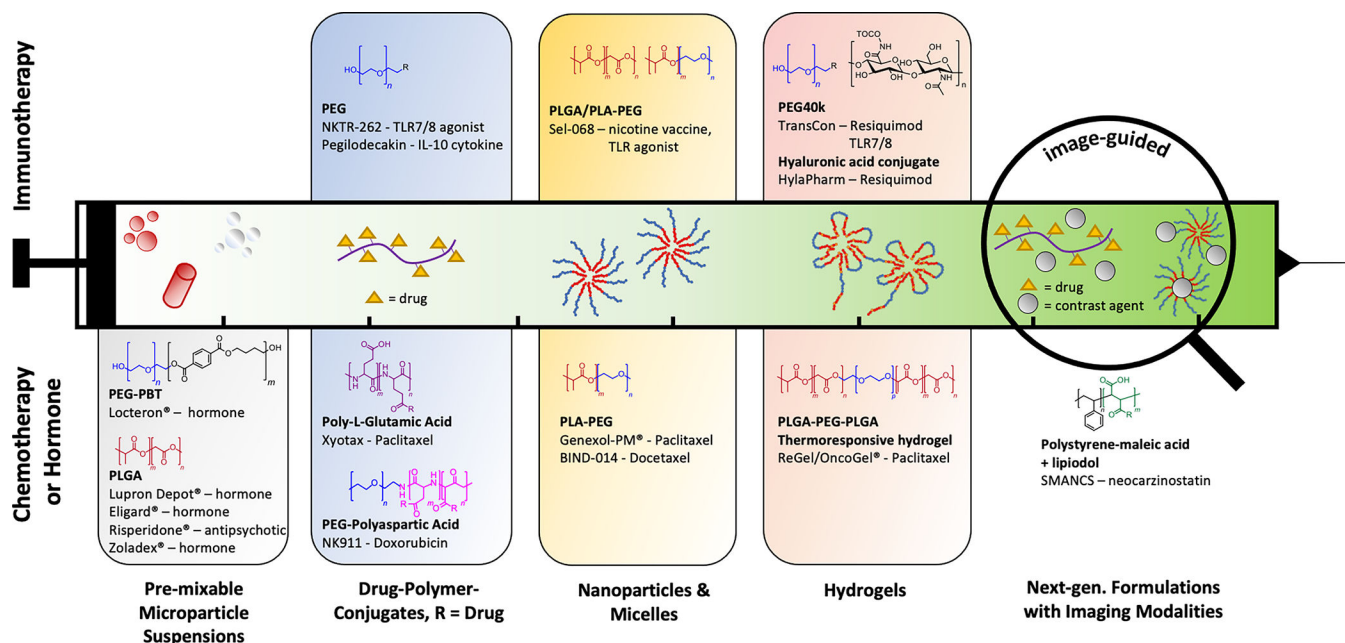
**Figure 1.** Mechanisms of immunotherapy. From left to right, in a recruitment phase cytokines, TLR-9 agonists, STING agonists, etc, induce IFN- $\gamma$  release locally leading to dendritic cell recruitment and activation in the tumor region. In the middle, priming phase, these dendritic cells activate T-cells, and where anti- CTLA-4 antibodies block T-cell and dendritic cell inhibitory signals, allow activation. Subsequently PD-1 agonists inhibit inhibitory signals from the tumor cells. Created with [BioRender.com](https://www.biorender.com).



**Figure 2.** (Graphical abstract). Mechanism of image guided intra-tumoral immunotherapy and abscopal effect. From left to right, CT or ultrasound are clinically practical ways to inject deep lesions with an immunotherapy controlled release depot that contains a contrast agent for visualization, the resultant treated lesion leads to cytokine release, dendritic cell recruitment and antigen that is picked up by dendritic and macrophage tissues. This material is taken to a draining lymph node where (middle figure) an antigen presenting cell presents to a T – cell to be activated. Right figure, an activated T-cell then subsequently induces apoptosis in distant cancer such as in the lung. Created with [BioRender.com](https://www.biorender.com/).

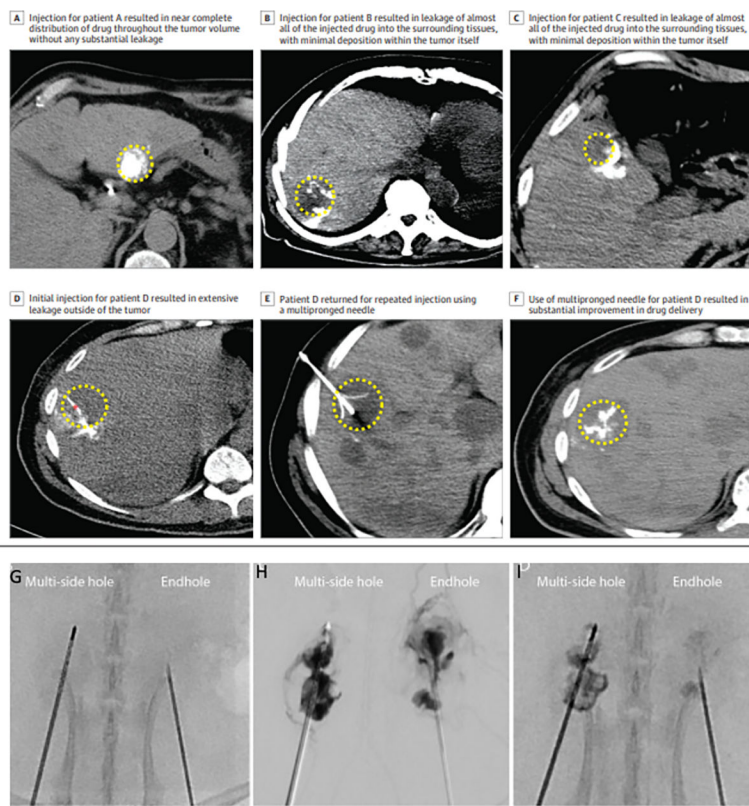


**Figure 3.** Clinical trials of intra-tumoral immunotherapies. a) Stages of ongoing clinical trials related to the injection-based delivery of intra-tumoral immunotherapy agents. Data from [clinicaltrials.gov](https://clinicaltrials.gov) as of July 2021. b) Tumor types addressed in these clinical trials.



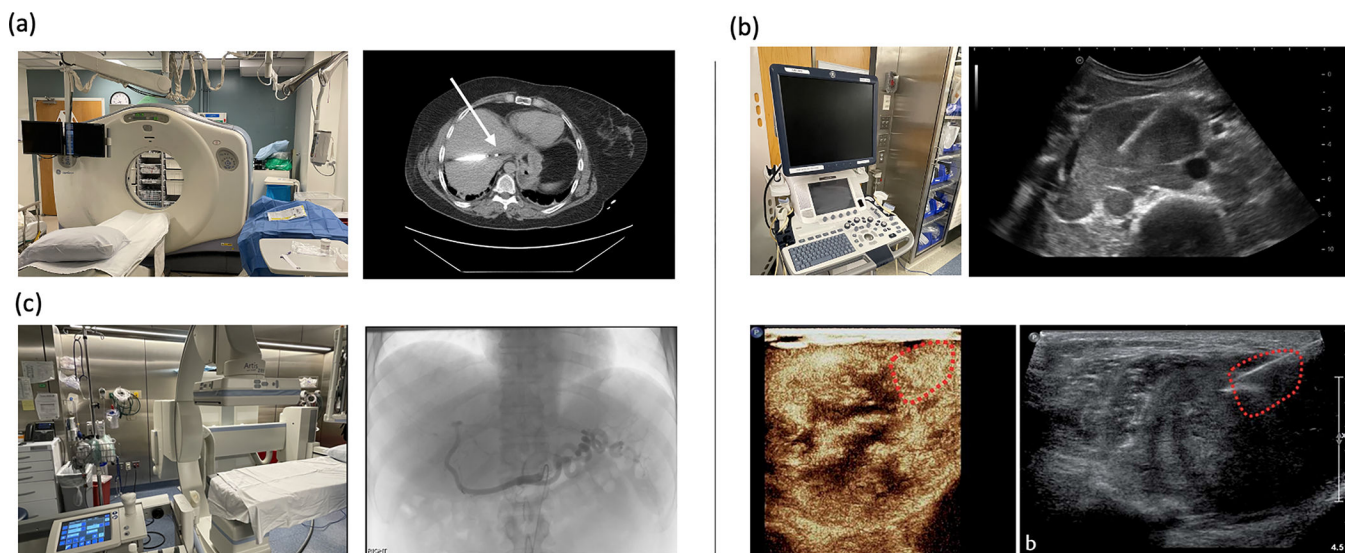
**Figure 4.**

Examples of commercially relevant injectable polymer-based drug release formulations for chemotherapy (lower half) and immunotherapy (upper half). First injectable formulations in the 1980's were mostly based on degradable and non-degradable microparticle suspensions (1<sup>st</sup> block from left). On the nanoscale, functional groups on the polymer backbone (such as polycarboxylic acid polymers) or at the end groups (typically PEG) can be used to make drug-polymer-conjugates that can reduce systemic toxicity and increase target accumulation (2<sup>nd</sup> block). Amphiphilic block-copolymers such as PEG-PLA's will self-assemble around hydrophobic drugs, enabling improved target uptake through decoration of target-specific functionalities on the resulting corona surface (3<sup>rd</sup> block). Hydrogels are another platform technology to facilitate encapsulation, injectability, local retention and extended release of chemo and immunotherapy agents, through either medium- to long-chain viscosity increasing polymers, such as PEG or hyaluronic acid, or stimuli-responsive gelling copolymers such as PLGA-PEG-PLGA. Towards the paradigm of personalized medicine, implementing imaging modalities and thus the live trackability of an injected payload is a desired feature of the future for which not many examples exist yet. Adapted with permission from Kamaly et al. Copyright 2016 and modified. American Chemical Society [29]



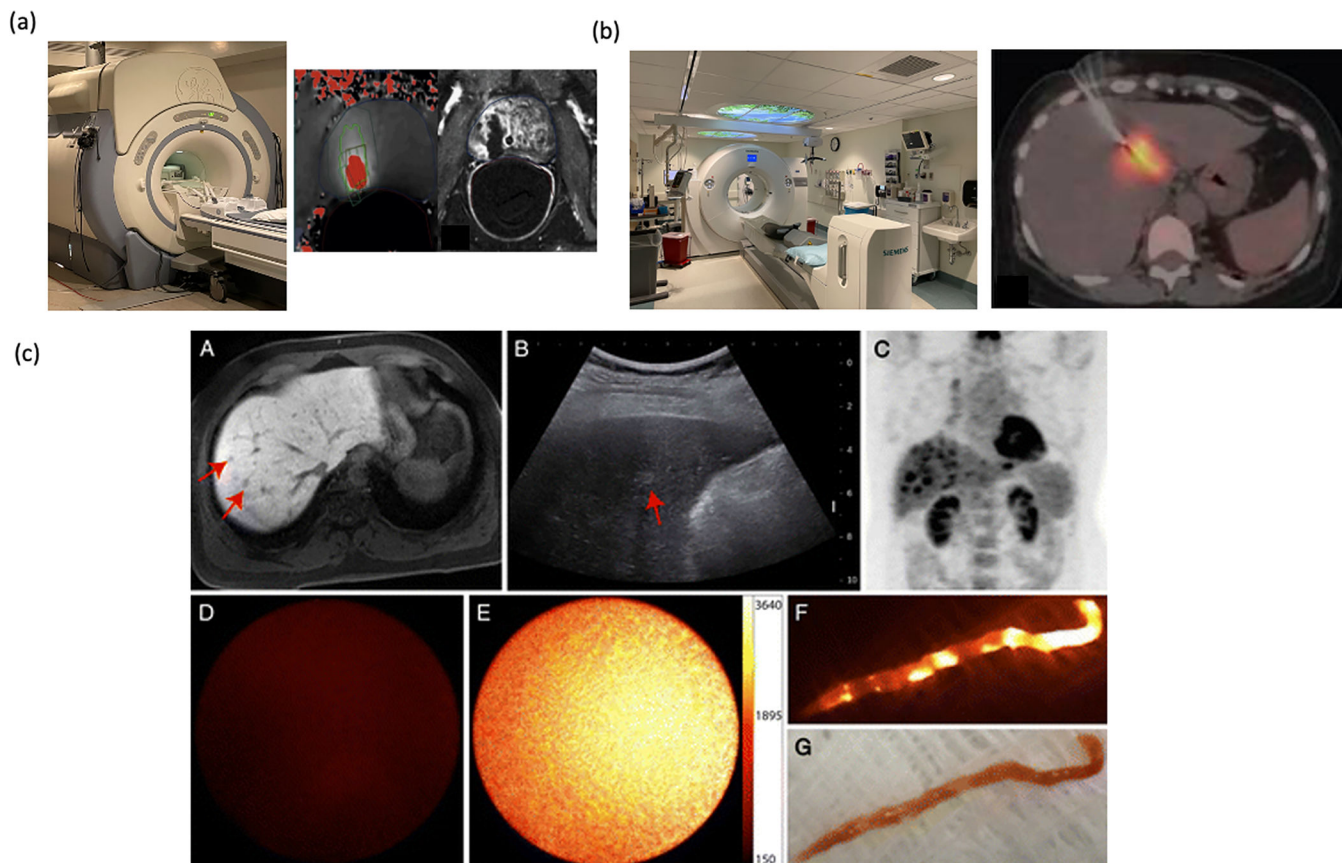
**Figure 5.**

Original figure a-f adapted from Sheth, et. al. JAMA Open, Creative Commons, used with permission. [17] a) Demonstration of injection distribution in a patient throughout the tumor. b-d) Demonstration of injection leaking out of the tumor. e) Injection using a multi-prong injection needle f) contrast demonstrating better injection distribution from the multi-prong injection. g) Side by side comparison of a multi-side hole versus end hole needle injection in a kidney animal model. h) Injection side by side shows more uniform distribution with the multi-side hole. i) Better retention is seen post injection with the multi-side hole. Images in g,h,i reproduced with permission from the work by Munoz et. al. 2021, Creative Commons License. [44]



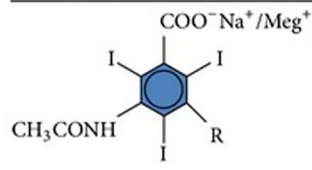
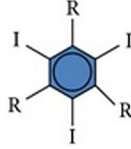
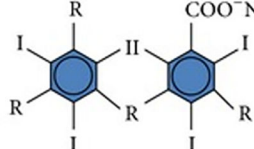
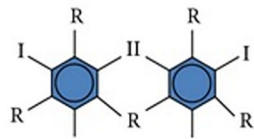
**Figure 6:**  
 Practical clinical imaging modalities and example clinical image of a procedure. a) CT apparatus and image of a microwave probe in a hepatocellular lesion. b) Ultrasound device, and ultrasound image of an ultrasound guided biopsy. Contrast enhanced ultrasound with biopsy of a proven melanoma metastasis. Bottom two images reproduced with permission from Kopf et. al. Copyright European Journal of Ultrasound. [161] c) Fluoroscopy suite with angiographic image demonstrating selective catheterization of the celiac artery during a trans arterial chemoembolization.



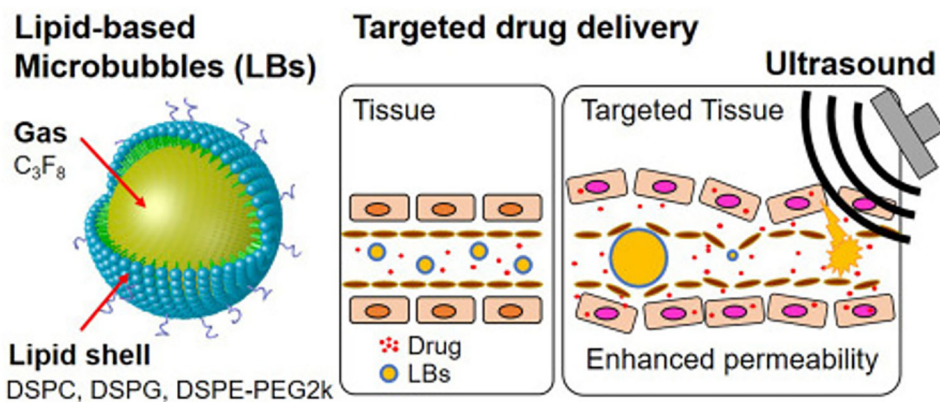


**Figure 7.** Uncommon clinical imaging modalities. a) MRI machine, and MR guided focal ultrasound ablation showing MR thermometry and area of ablation. Adapted with permission from Napoli et. al. Copyright European Urology[105] b) PET- CT, PET guided biopsy of a liver lesion, Adapted from Govindarajan, et. al. Creative Commons License [108]. c) Use of near infrared imaging to confirm biopsy specimen subpart A shows lesion on MRI, subpart B shows on ultrasound, subpart C shows FDG avidity, sub-part D shows no fluorescence on normal liver, sub-part E shows fluorescence during active guidance in sub-part E, and fluorescence on external imaging, sub-part F, and corollary visuals in sub-part G. Images reproduced with permission from Sheth et. al. Radiology 2014 Copyright Radiology.[109]

(a)

Molecular structure	Era	Examples	Comment
	1950s	Ionic monomer Diatrizoate Iothalamate	High osmolality, 5–8x blood
	1980s	Nonionic monomer Iopamidol Iohexol Ioversol	Low osmolality, 2–3x blood, improved hydrophilicity
	1980s	Ionic dimer Ioxaglate	Low osmolality, ~2x blood
	1990s	Nonionic dimer Iodixanol (iotrolan)	Isoosmolality Osmolality = blood

(b)

**Figure 8:**

a) Various iodinated contrast agents and their structure, reproduced from Solomon, et. al. Creative Commons License [110] b) lipid microbubbles, reprinted with permission from Elsevier, adapted from Omata, et. al. 2020 [112]

**Table 1:**

Currently available anti-PD-1 and Anti-CTLA-4 immunotherapies, table adapted from Seidel et. al. “Anti-PD-1 and Anti-CTLA-4 Therapies in Cancer: Mechanisms of Action Efficacy, and Limitations. Creative Commons License [3]

Target	Drug	Condition	Objective Response Rate	Complete Response Rate	Overall Survival (months)	Participants	Reference
PD-1	Nivolumab	Melanoma	43.70%	8.90%	n/a	316	[133]
		RCC (metastatic)	25% (4% Control)	1% (<1% control)	25.0 (19 control)	406 (397 control)	[134]
		Hodgkin’s Lymphoma	87%	17%	n/a	23	[135]
		SCC - Head and Neck	13.3% (5.8%)	2.5% (0.8% control)	36%/ 1 year (16.6% control)	240 (121 control)	[136]
		NSCLC	19% (12% control)	1% (<1% control)	12.2 (9.4 control)	292 (290 control)	[137]
	Pembrolizumab	Ovarian Cancer	15%	10%	20	20	[138]
		Melanoma	33.7–32.9%	5–60.1%	n/a	279–277	[139]
		Merkel cell carcinoma	56%	16%	n/a	26	[140]
		Non-small cell lung cancer	19.40%	n/a	12	495	[141]
		Progressive metastatic colorectal carcinoma	40%	0	>5 months/ 5	10 (18 control)	[142]
Pidlizumab	B cell lymphoma	51%	34%	85% at 16 months	66	[143]	
	Follicular lymphoma	66%	52%	n/a	29	[144]	
Anti-CTLA4	Ipilimumab	Melanoma (stage III/IV)	15.2% (10.3% control)	1.6% (0.8% control)	11.2 (9.1 control)	250 (252 control)	[145]
	Tremelimumab	Melanoma (stage III/IV)	10.7% (9.8% control)	3% (2% control)	12.6 (10.7 control)	326 (327 control)	[146]
Combination Therapy	Nivolumab + Ipilimumab	Melanoma (stage III/IV)	57.60%	11.50%	n/a	314	[133]
		Small cell lung cancer (recurrent)	23%	2%	7.7	61	[147]

**Table 2**

Studies investigating controlled release of Immunotherapy and Immunoadjuvants. Adapted with copyright permission of tables originally presented by Huang, et. al. Nano, micro-, and macroscale drug delivery systems for cancer immunotherapy. Copyright Elsevier. [59]

Therapy Route	Scale	Immunotherapy	Formulation	Duration of Release	Animal Outcomes	Imaging	Ref
Surgical Implantation into the tumor resection bed	Macroscale	Tumor lysate + TLR3 agonists, gemcitabine	Cross-linked collagen and hyaluronic acid scaffold - implanted as a 5 mm disc	40% plateau release in 6 days of the nano-gel, and release of 4T1 lysate over 30 days,	increase DC, enhance T- cells, IFN- $\gamma$ , resolution of lung metastasis compared to control surgery, vaccine alone, or gemcitabine	Not applicable	[64]
Direct injection in the tumor bed	Nanoscale	CpG ODN, Anti-PD-1 antibody	CpG Nano-Cocoon	Activation of macrophages by 6 hours.	Increased survival time of mice in post- surgery, with direct injection in the tumor bed	None	[79]
Intratumoral injection	Microscale	anti-CTLA4	Ethiodized oil and poly-lactic-co-glycolic acid nanoparticles (PEEP)	30-day release to plateau	Improvement in survival in CT-26 tumors, similar with direct anti-CTLA4 and with PEEP.	Radio-opaque, ethiodized oil	[60]
Intratumoral injection	Macroscale	Anti-PD-1 antibody, IDO Inhibitor	P(Me-D-1MT)-PEG-P(Me-D-1MT) Hydrogel	25% release at 4 days prerelease, and near 100% release with ROS by 24 hours. aPD-L1 seen up to 7 days in vivo as opposed to free aPD-L1(3–5 days)	Decreased systemic toxicity and enhanced anti-tumor t-cell immature response, reduced tumor growth in vivo	Fluorescence	[61]
Intratumoral injection	Nano-macroscale	STING agonist + Camptothecin	Peptide drug moiety iRGD+camptothecin - supramolecular nanotubes + STING agonist (c-di-AMP)	Retention drug release out to 15 days in vivo	Reduced tumor growth and regression in GL-261 brain tumors.	Fluorescence - FITC	[62]
intratumoral injection	Macroscale	OX40 and CD40	Nanofluidic membrane with multiple channels from patterned tungsten layer created via physical vapor deposition. Lyophilized antibody solubilizes in the fluid and pushes out by diffusion	30-day release	Inhibition of tumor growth (4T1 orthotopic murine tumor)	None	[63]
IV injection	Nanoscale	IDO inhibitor, DPPA-1	Self-assembling D-peptide programmed cell death ligand 1	80% release in 4 hours in tumor mimicking environment (pH 6.8 + MMP), 20% release > 48 hours in pH 7.4	sensitive to MMP-2, slowed melanoma growth and inc'd CD8+ T cells	None	[66]

Therapy Route	Scale	Immunotherapy	Formulation	Duration of Release	Animal Outcomes	Imaging	Ref
IV injection	Nanoscale	TGF-B inhibitor, IL-2	Nanoscale liposomal polymeric gel	7 days	IV injection- Increased efficacy compared to solubilized drug alone. Treatment every 7 days for 40 days.	Fluorescence - rhodamine	[67]
IV injection	Micro/ Nanoscale	CpG oligonucleotide with TRP2 peptide	Porous silicon microparticles (500–1000 nm)	Majority release in 20 hours and remainder by 100 hours, cleared in vivo by 72 hours, primarily in liver and lungs	Co-delivery of two different TLR Agonists (CPG oligo nucleotide and MPLA increased CD8 response against B 16 melanoma). Mildly increased survival in B16 melanoma (1/8) to 60 days	Fluorescence	[148]
IV injection	Nanoscale	Imiquimod (TLR - 7 agonist)	PLGA-ICG- Imiquimod	N/A (Biological effect within 7 days)	Photoacoustic + immunotherapy effect inhibitors growth	Fluorescence	[69]
Intradermal injection	Macroscale	OVA, CpG	CpG DNA hydrogel	20–50% release of OVA by 24 hours in vitro, and near 100% release by 24 hours, as compared to less than 6 in vivo	Cationized antigen reduced tumor growth in vaccinated subgroups compared to control without the gel on tumor challenge	Fluorescence	[70]
Subcutaneous injection in the hind footpads of mice	Nanoscale	OVA, TLR-7/8a	N-(2-hydroxypropyl) methacrylamide (HPMA) and N-isopropylacrylamide (NIPAM) covalently conjugated to TLR-7/8a	Persisted up to 20 days	Increase cytokine production in lymph node with particles, compared to free drug	Fluorescence	[71]
Subcutaneous implantation	Microscale	Anti-CD137, anti-OX40 mAb in a hybridoma	Alginate-Ca microparticles	Majority in 1-week, complete loss by 14 days	Alginate-Ca microparticles encapsulated with hybridomas result in increased in cytotoxic T-cell lymphocyte response with 4–6/7 complete eradication of CT-26 models	N/A	[72]
Subcutaneous injection	Macroscale	Tumor vaccine CpG - ODN, GM-CSF	Mesoporous silica rod scaffold	66% release of GM-CSF by day 40, OVA 45% release in 5 days, sig increased from free OVA	Scaffold induces dendritic cell recruitment and increases cytotoxic t- cells, and allows adjuvant release	Fluorescence	[73]
Subcutaneous injection	Microscale	PLGA particle containing CpG-ODN and Ovalbumin	PLGA microparticles	Highest peak IgG titer at day 56, and IFN- $\gamma$ persisting until day 42, PLGA fluorescence down to near zero by 20	Increased cytotoxic T cell response and interfered with tumor growth.	Fluorescence	[74]

Therapy Route	Scale	Immunotherapy	Formulation	Duration of Release	Animal Outcomes	Imaging	Ref
Subcutaneous injection, tail base	Nanoscale	CpG Neo-antigen	Lipoprotein-mimicking nanodisc	Peak 28 hours, and reduced by 48 hours (compared to < 10 hours control) - cell culture	47-fold greater neo-antigen-specific CTLs than soluble vaccines, eliminating MC-38 and B16F10 tumors, 30 % Glioma	Fluorescence	[75]
Subcutaneous injection, tail base	Microscale	OVA or TCL	Yeast-derived microparticles	N/A	Increased DC triggered antigen delivery. detected OVA antibody post injection, followed by subsequent tumor (lymphoma) challenge showing improvement with YS-OVA vs either alone or with alum	Fluorescence-FITC	[76]
Subcutaneous injection, tail base	Macroscale	Tumor cell lysates, TLR 3 agonist, poly(I:C)	PEG-poly(L-Valine) hydrogel	Cumulative release to 80 % by 120 hours. Burst release to 40% in 1 day	Modulate antigen specific immunity	Fluorescence	[77]
Subcutaneous, intrascapular region	Macroscale	E7 peptide, B16F10 or CT-26 neoantigens	Mesoporous silica rod scaffold-Polyethyleneimine	Not studied.	Neoantigens-eliminated established lung metastasis in TC-1 B16F10 and CT -26 mice synergized with anti-CTLA4 therapy	Not applicable	[78]



**Table 3**

Summary of imaging modalities used in a variety of hydrogel delivery agents. Adapted with copyright permission from Dong, et. al. "Detecting and monitoring hydrogels with medical imaging". Copyright 2021 American Chemical Society [114]

Imaging modality	Imaging functionalization	Polymer	Drug Delivery	Drug Release Duration	Contrast Duration	Ref
CEST-MRI	Intrinsic	Alginate/Liposome	--	--	Duration of polymer	[116]
CEST-MRI	Intrinsic	Hyaluronic acid-SH/ gelatin-SH (Can then be labeled with NIR days as well).	--	--	Duration of polymer	[117]
CEST-MRI	Intrinsic	Peptide-conjugate (glutamic acid + phenylalanine)	--	--	Duration of polymer	[118]
CT	Gold Nanoparticles	Gelatin-Tyramine	N-acetyl cysteine			[127]
CT	Gold Nanoparticles	Alginate	Cisplatin	minimum 7 days (unsure)	--	[149]
CT	Gold Nanoparticles	PNAGA-PAAM copolymer N-acryloyl glycinamide	Doxorubicin	24 hrs	minimum 48 hr	[128]
CT	iopamidol and tantalum-oxide particles	gelatin-tetrazine/gelatin -norbornene	--	--	minimum 12 days (Ta- gel)	[150]
CT	Platinum nanoparticles	alginate	--	--	minimum 5 days (experiment did not continue beyond this; 80% Pt loss in DOHEPTs at this time point)	[65]
CT	Gold Nanoparticles	Selenocystamine - poly(bis(4- carboxyphenoxy) phosphazene)) (Se PCPP)	doxorubicin, quisinostat, etc.)	70% release in 7 days with XR		[151]
CT	Iodinated trimethylene carbonate	PLGA-PEG-PLGA with co-polymer of the iodinated trimethylene carbonate	--	--	24 days for 100% released	[129]
CT	Ethiodized Oil	Ethiodized oil and poly-lactic-co-glycolic acid nanoparticles (PEEP)	anti-CTLA-4	30-day release to plateau	Not tested	[60]
CT	Barium sulfate suspensions in hydrogel microcoils	Polyacrylonitrile	--	--	minimum 12 weeks (experiment did not continue beyond this)	[152]
CT	2,3,4-triiodobenzoic acid	Poly (ethylene glycol) and aliphatic polyester coupling the hydroxyl end of the diblock copolymer with 2,3,5- triiodobenzoic acid (TIB)	--	--	5–7 days (little left at in vivo in mouse abdomen; no gel visible at 7 days)	[153]
<b>CT &amp; Optical</b>	Ta <sub>2</sub> O <sub>5</sub> India Ink	Gelatin functionalized with tetrazine/ norbornene	--	--	Stability for up to 12 days <i>in vivo</i>	[154]
Fluorescence	Intrinsic	Polyacrylamide	--	--	Duration of polymer	[119]
Fluorescence	Intrinsic	BSA/HAS	--	--	Duration of polymer	[120]

Imaging modality	Imaging functionalization	Polymer	Drug Delivery	Drug Release Duration	Contrast Duration	Ref
Fluorescence	Carbon Nanodots	N-methacryloyl chitosan	--	--	minimum 500 hr (experiment did not continue beyond this)	[122]
Fluorescence	Indocyanine Green	RADA16-I peptide	Melittin	2 days (at least; experiment did not continue beyond this)	2 days (ICG contrast had slower release than melittin, reaching 20% release rate at 2 days, while melittin reached 40%; at least; experiment did not continue beyond this)	[155]
Fluorescence	Quantum dots	Fmoc-diphenylalanine	--	--	minimum 5 hr (experiment did not continue beyond this)	[125]
Fluorescence/ photoacoustic	Ag2S quantum Dots	polypeptide PC10	Paclitaxel	6 days	35 days	[121]
fluorescence/M RI/ultrasound	rhodamine B and CoFe2O4	PLGA-PEG-PLGA	Luciferin (as a model for small molecule delivery)	7 days; liposomes remain stable in vivo for 3 weeks and release drug upon heating triggered by laser light (42 C)	20 mins (can be reactivated upon reheating)	[126]
Fluoroscopy	iodinated contrast agents	chitosan	--	--	at 4 h, decreased 80% [Conray], 56% [Visipaque] and 68% [Isovue]	[130]
Fluoroscopy	iohexol	PEGDA/ Alginate	--	--	--	[131]
MRI	M-Ferrite nanoparticles	AM PEG550	Paclitaxel	28 days (at least; at which 71.16 ±13.34% of initial amount put in gel was released)	28 days (93.68 ± 1.06% of initial amount put in gel released)	[156]
MRI	DOTA-GD(III)	Polyethylene - Glycol	--	--	minimum 2 wks (only 23% of Upy-Gd was released at this point)	[157]
MRI	ferumoxytol	Chitosan	Doxorubicin	16 hr	40 hr	[158]
SPECT/CT	Ba2+In3+Zr4+	Alginate	--	--	8 days in nose (function of mucus clearance; different duration when hydrogel is injected into different body parts)	[159]
SPECT/CT	99mTc	Carboxymethyl- cellulose	Pheonix WinNonlin (1- compartmental model)	--	--	[160]
Ultrasound	SonoVue microbubbles	silk fibrin	--	--	minimum 7 days (experiment did not continue beyond this)	[132]